The lithospheric architecture of Africa: Seismic tomography, mantle petrology, and tectonic evolution

G.C. Begg
Minerals Targeting International, 26/17 Prowse Street, West Perth, Western Australia 6005, Australia, and GEMOC ARC National Key Centre, Department of Earth and Planetary Sciences, Macquarie University, New South Wales 2109, Australia

W.L. Griffin
L.M. Natapov
Suzanne Y. O'Reilly
GEMOC ARC National Key Centre, Department of Earth and Planetary Sciences, Macquarie University, New South Wales 2109, Australia

S.P. Grand
Jackson School of Geosciences, University of Texas at Austin, Austin, Texas 78712, USA

C.J. O'Neill
GEMOC ARC National Key Centre, Department of Earth and Planetary Sciences, Macquarie University, New South Wales 109, Australia

J.M.A. Hronsky
Western Mining Services (Australia), 26/17 Prowse Street, West Perth, Western Australia 6005, Australia

Y. Poudjom Djomani
GEMOC ARC National Key Centre, Department of Earth and Planetary Sciences, Macquarie University, New South Wales 2109, Australia, and Geological Survey of New South Wales, Maitland, New South Wales 2320, Australia

C.J. Swain
Western Australian Centre for Geodesy, Curtin University of Technology, Perth, Western Australia 6845, Australia

T. Deen
GEMOC ARC National Key Centre, Department of Earth and Planetary Sciences, Macquarie University, New South Wales 2109, Australia, and British Antarctic Survey, High Cross, Madingley Road, Cambridge CB3 0ET, UK

P. Bowden
Department of Geology-Petrology-Geochemistry, Université Jean-Monnet, 42023 Saint-Étienne, France

ABSTRACT

We present a new analysis of the lithospheric architecture of Africa, and its evolution from ca. 3.6 Ga to the present. *Upper-lithosphere domains*, generated or reworked in different time periods, have been delineated by integrating regional tectonics and geochronology with geophysical data (magnetic, gravity, and seismic). The origins and evolution of *lower-lithosphere domains* are interpreted from a high-resolution global shear-wave tomographic model, using thermal/compositional modeling and xenolith/xenocryst data from volcanic rocks. These data are integrated to map the distribution of ancient highly depleted subcontinental lithospheric mantle (SCLM), zones of younger or strongly modified SCLM and zones of active mantle upwelling, and to relate these to the evolution of the upper lithosphere domains.

The lithospheric architecture of Africa consists of several Archean cratons and smaller cratonic fragments, stitched together and flanked by younger fold belts; the continental assembly as we see it has only existed since lower Paleozoic time. The larger cratons are underlain by geochemically depleted, rigid, and mechanically robust SCLM; these cratonic roots have steep sides, extending in some cases to ≥300-km depth. Beneath smaller cratons (e.g., Kaapvaal) extensive refertilization has reduced the lateral and vertical extent of strongly depleted SCLM. Some cratonic roots extend ≥300 km into the Atlantic Ocean, suggesting that the upper lithosphere may detach during continental breakup, leaving fragments of SCLM scattered in the ocean basin.

The cratonic margins, and some intracratonic domain boundaries, have played a major role in the tectonics of Africa. They have repeatedly focused ascending magmas, leading to refertilization and weakening of the SCLM. These boundaries have localized successive cycles of extension, rifting, and renewed accretion; the ongoing development of the East Africa Rift and its branches is

Geosphere; February 2009; v. 5; no. 1; p. 23–50; doi: 10.1130/GES00179.1; 17 figures; 2 animations.

only the latest stage in this process. The less depleted SCLM that underlies some accretionary belts may have been generated in Archean time, and repeatedly refertilized by the passage of magmas during younger tectonic events. Our analysis indicates that originally Archean SCLM is far more extensive beneath Africa than previously recognized, and implies that post-Archean SCLM rarely survives the collision/accretion process. Where continental crust and SCLM have remained connected, there is a strong linkage between the tectonic evolution of the crust and the composition and modification of its underlying SCLM.

INTRODUCTION

The lithosphere is the outermost, relatively rigid shell of the Earth, made up of the crust and the underlying lithospheric mantle. Beneath the continents, the subcontinental lithospheric mantle (SCLM) varies widely in thickness, from a few tens of kilometers beneath active rift zones to >250 km beneath some ancient cratonic blocks. The SCLM, as sampled by xenoliths in volcanic rocks and some exposed massifs, consists almost entirely of peridotitic rocks (olivine + orthopyroxene ± garnet ± clinopyroxene ± spinel). Re-Os isotopic studies show that beneath some Archean cratons, the SCLM is at least as old as the oldest known crustal rocks (Carlson et al., 1999; Griffin et al., 2004; references therein).

From studies of mantle-derived xenoliths and the distribution of diamonds, Janse (1994) recognized that the nature of the SCLM is related to the tectonothermal age of the overlying crust, as defined by the timing of the last major tectonothermal event. We will use a modification of Janse's terminology, in which the last major crustal tectonothermal event in *Archons* occurred at ≥2.5 Ga, in *Protons* between 2.5 and 1 Ga, and in *Tectons* at <1 Ga.

Data from xenoliths and exposed massifs show a marked secular evolution in SCLM composition, broadly related to the tectonothermal age of the overlying crust (Griffin et al., 1998, 1999; O'Reilly et al., 2001). *Archon* SCLM is strongly depleted in basaltic components, with highly magnesian olivine and pyroxenes, whereas *Tecton* SCLM is only mildly depleted relative to estimates of primitive mantle compositions; *Proton* SCLM tends to be intermediate between these two extremes. The secular evolution of the SCLM may reflect changes in the processes that produce juvenile SCLM, or the progressive refertilization of old SCLM, or both (Griffin et al., 2003b; Beyer et al., 2006). Regardless of the interpretation, this broad correlation between crustal history and SCLM composition implies a strong linkage between crust and mantle, and the processes affecting both, over time spans measured in eons.

The secular evolution of SCLM composition has major consequences for the nature of crustal tectonics through time. Archon SCLM is buoyant relative to the underlying asthenosphere, and this buoyancy may have played an important role in the stabilization of cratons (Poudjom Djomani et al., 2001). Tecton SCLM, being less depleted, is buoyant relative to the asthenosphere as long as its geotherm remains elevated, but on cooling it is likely to become unstable, and may delaminate and sink. At some convergent margins, crustal thickening and the transformation of mafic lower crust to eclogite may result in a more continuous drip-style of lithosphere removal (e.g., Sobolev et al., 2005). In either case, the ensuing upwelling of asthenospheric material can lead to widespread crustal melting, as in the Central Asian Orogenic Belt (Zheng et al., 2006; references therein). Refertilization of older SCLM by asthenosphere-derived melts leads to an increase in SCLM density, enhancing the probability of delamination. The nature and history of the SCLM therefore will affect the response of the overlying crust to tectonic stresses. Lithospheric architecture, and particularly the presence of boundaries between domains with different types of SCLM, will be important in controlling crustal tectonics, and especially the transport of fluids and magmas from depth. This control may have important implications for the distribution of major ore deposits; an understanding of crust-mantle linkages and lithospheric architecture therefore has direct economic relevance.

Most of our detailed knowledge of SCLM composition comes from the study of xenoliths and xenocrysts brought up in volcanic rocks (Griffin et al., 1999; O'Reilly and Griffin, 2006; references therein). However, these samples are scattered in time and space, and are not available for large areas of the continents. To map the SCLM, and to understand its evolution, we must turn to geophysical data, and learn to interpret these data in terms of SCLM composition and evolution.

In this paper we integrate high-resolution (275-km lateral cell size) global seismic tomography with data on crustal tectonic history and mantle petrology, to map the distribution of different SCLM types under Africa. Our aim is to understand the relationships between the three-dimensional lithospheric architecture of the continent and its tectonic history; on a broader scale, this approach provides insights into the fundamental processes controlling the assembly and breakup of continents through time.

REGIONAL GEOLOGY AND TECTONICS OF AFRICA—AN OVERVIEW

This brief review of the complex basement geology of Africa (Fig. 1) focuses primarily on the timing and nature of major tectonothermal events that have affected specific areas. It is intended to provide a background for examining correlations between mantle composition, the geophysical signature of the SCLM, and the evolution of the overlying crust. Details of age relationships and alternative structural interpretations have necessarily been subordinated to this larger aim. To simplify reading, key references are gathered at the beginning of each section.

Since late Proterozoic time, Africa has been a center of continental accretion. Today it is surrounded on three sides by divergent plate boundaries; despite minor compression on its northern edge, it is essentially stationary. Global seismic tomography and geodynamic modeling suggests that it sits atop a major mantle upwelling, the African Superswell, and is beginning to break apart along the East Africa Rift Zone (Grand et al., 1997; Nyblade and Langston, 1998; Lithgow-Bertelloni and Silver, 1998; Ritsema et al., 1998, 1999; Gurnis et al., 2000; Kieffer et al., 2004; Simmons et al., 2007).

Archean Cratons (Archon, Proton/Archon, and Tecton/Proton/Archon)

The basic fabric of Africa (Fig. 1) consists of several major Archean cratons and smaller cratonic fragments, stitched together and flanked by younger fold belts; the framework of the modern continent was established in the Late Neoproterozoic to earliest Paleozoic Pan-African orogenic event. The cratons themselves are aggregates of continental fragments 3.6–2.5 Ga in age, and differ markedly from one another in their structure and evolution.

West African Craton (Cahen et al., 1984; Boher et al., 1992; Goodwin, 1996; Potrel et al., 1996; Attoh and Ekwueme, 1997; Kouamelan et al., 1997)

The West African Craton is largely covered by the Neoproterozoic to Paleozoic Taoudeni Basin. Archean rocks are exposed in the Reguibat Shield on the north side and the Man-Leo Shield on the south; strong similarities between them suggest that the shields are part of a larger craton that underlies the Basin. Migmatitic orthogneisses (3.5 Ga) and greenstone belts (3.3–3.1 Ga) in the western parts of the shields were affected by granulite-facies metamorphism at ca. 2.9–2.7 Ga. A significant part of these

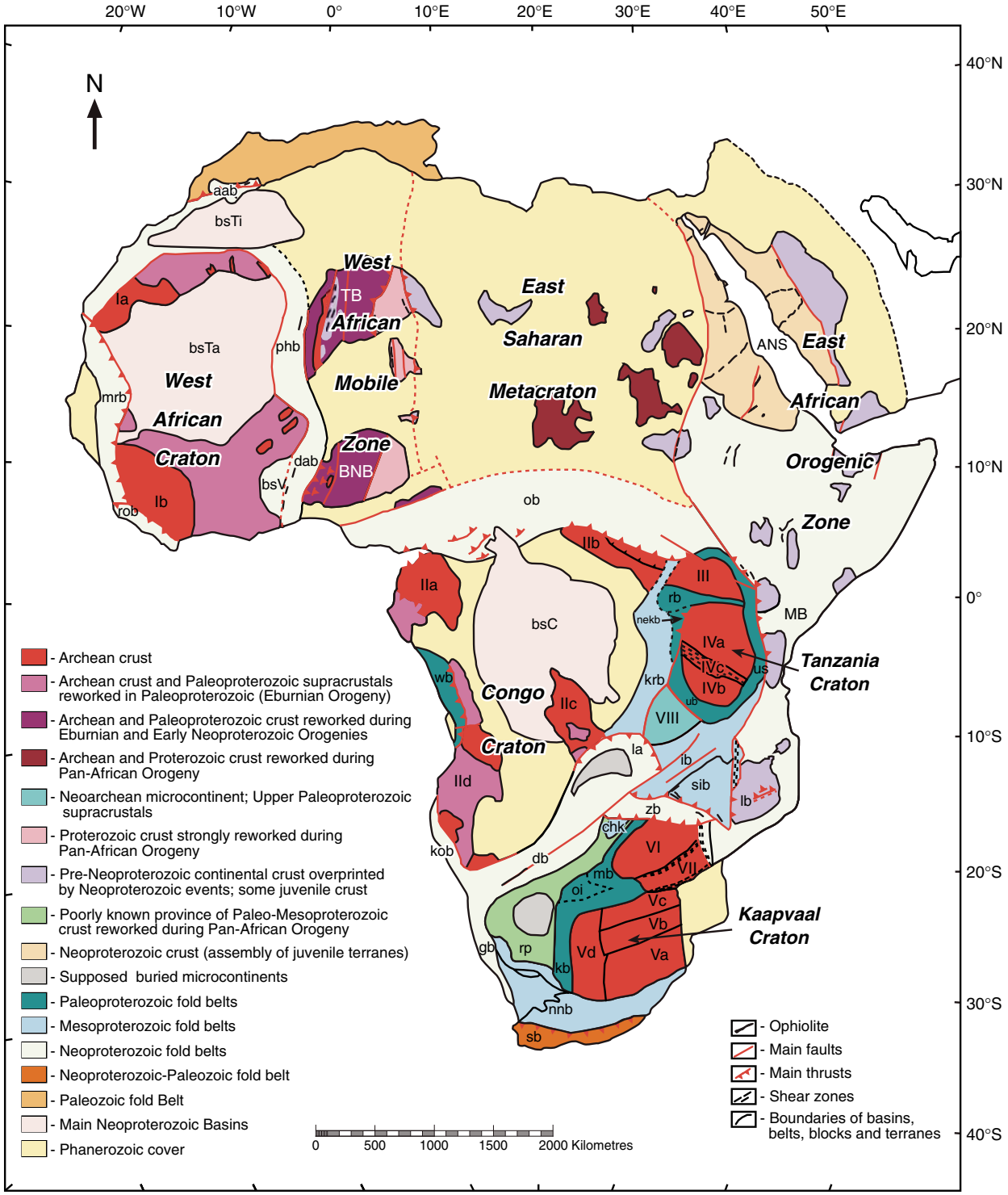

Figure 1. Map of the bedrock geology of Africa, outlining the major subdivisions of the crust discussed in the text. Cratons and Microcontinents: West African Craton (Ia—Reguibat Shield; Ib—Man-Lèo Shield); Congo Craton (IIa—Gabon-Kamerun Shield; IIb—Bomu-Kibalian Shield; IIc—Kasai Shield; IId—Angolan Shield); Ugandan Craton—III; Tanzanian Craton (IVa—Northern Terrane; IVb—Southern Terrane; IVc—Dodoma Zone); Kaapvaal Craton (Va—Southern Terrane; Vb—Central Terrane; Vc—Pietersburg Terrane; Vd—Western Terrane); Zimbabwe Craton—VI; Limpopo Block—VII; Bangweleu Block—VIII. West African Mobile Zone: TB—Tuareg Block; BNB—Benin-Nigerian Block. East African Orogenic Zone: ANS—Arabian-Nubian Shield; MB—Mozambique Orogenic Belt. Fold Belts: *Paleoproterozoic Belts:* ub—Ubendian; us—Usagaran; rb—Ruwenzory; kb—Kheis; oi—Okwa inlier; mb—Magondi; wb—West Central African; nekb—North-Eastern Kibaran. *Paleo-Mesoproterozoic Province*: rp—Rehoboth. *Mesoproterozoic Belts:* krb—Kibaran; ib—Irumide; sib—Southern Irumide; chk—Chomo-Kolomo; nnb—Namaqua-Natal. *Neoproterozoic Belts:* zb—Zambezi; la—Lufilian arc; db—Damara; kob—Kaoko; gb—Gariep; ob—Oubanguides; aab—Anti-Atlas; phb—Pharusian; dab—Dahomeyean; rob—Rockellides; mrb—Mauritanides; lb—Lurio; sb—Saldania. Neoproterozoic Basins: bsC—Congo; bsTa—Taoudeni; bsTi—Tindouf; bsV—Volta.

shields is covered by 2.2–2.1 Ga volcanic and sedimentary rocks of the Birrimian Supergroup, which were folded and intruded by granites during the 2.1–2.0 Ga Eburnian Orogeny.

Congo Craton
(Cahen et al., 1984; Walraven and Rumvegeri, 1993; Goodwin, 1996; De Carvalho et al., 2000; Tchameni et al., 2000)

Archean basement rocks are exposed in four shields located around the edges of the Congo Craton; marked differences in geological history among these shields suggest they represent separate terranes, but the terrane boundaries are not defined. The *Gabon-Cameroon Shield* in the NW corner of the craton contains 3.2–2.99 Ga migmatites, gneisses, and remnants of greenstone belts, cut by 2.97–2.54 Ga granites. The 2.15–2.05 Ga supracrustal cover rocks (Fransevillian Formation) are cut by 2.04–1.92 Ga granites. The *Bomu-Kibalian Shield* (NE edge) contains 3.42 Ga tonalitic gneisses and 3.0–2.6 Ga greenstone belts, as well as metamorphosed 2.51–2.46 Ga granites. The *Kasai Shield* (SE edge) is a heterogeneous 3.01 Ga granulite complex, metamorphosed at 2.9–2.6 Ga; it is overlain by metamorphosed supracrustal rocks, which were cut by granite plutons at ca. 2.1 Ga. The *Angolan Shield* (SW Angola) consists of gneisses, metasediments, and a 2.82 Ga gabbro-charnockite complex. The basement rocks were metamorphosed at 2.8–2.7 Ga and intruded by granites at 2.6 Ga. A Paleoproterozoic (2.15–2.1 Ga) cover sequence is cut by 2.1–2.0 Ga Eburnean granitoids.

Tanzanian Craton
(Borg and Shackelton, 1997; Manya and Maboko, 2003; Pinna et al., 2004; Schumann et al., 2004; De Waele, 2005)

This small Archean block consists of two terranes, joined along the NW-striking Dodoma Schist Belt, which is intruded by 2.6–2.5 Ga granites. The northern block has basement ranging from 2.8 to 2.66 Ga, overlain by a molasse that is intruded by 2.6 Ga granitoids. The southern block contains 2.93–2.85 Ga tonalite-trondhjemite-granodiorite (TTG) gneisses and associated granitoids. To the SW, the *Bangweulu Terrane* has limited exposures of Archean granites and supracrustal rocks, intruded by 2.73 Ga granitic rocks. The northern half of this terrane contains ca. 1.87 Ga arc-related metavolcanic rocks, 1.84–1.72 Ga gneisses and a ca. 1.8 Ga rift-related basin. The terrane is interpreted as a Neoarchean microcontinent, strongly affected by tectonic events in the surrounding Paleoproterozoic mobile belts.

Ugandan Craton
(Cahen et al., 1984; Schlüter, 1997; Schumann et al.,1999, 2004; Schenk et al., 2004; Loose et al., 2004; Appel et al., 2005)

Most of Uganda is underlain by Archean gneisses and granulites. The 2.9 Ga granulites in the western Nile area are intruded by 2.6–2.55 Ga granites. In the northwestern part of the craton, Archean granulites experienced ultrahigh pressure (UHT) metamorphism at ca. 2.4 Ga. This Archean block thus differs markedly from the Tanzanian Craton and the Bomu-Kibalian block of the Congo Craton. Its boundary with the Congo Craton is covered by the Neoproterozoic Oubanguides fold belt and sediments of the East African Rift Zone. Neoproterozoic cover and Archean rocks were reworked at 635–570 Ma.

Kalahari Craton
(Anhaeusser, 1990; Kröner Tegtmeyer, 1994; Goodwin, 1996; Blenkinsop et al., 1997; Brandl and de Wit, 1997; De Wit, 1998; Hofmann et al., 1998; Holzer et al., 1998; Frei et al., 1999; Kreissig et al., 2001; Dirks and Jelsma, 2002; Mapeo et al., 2004; Prendergast, 2004; Ramokate et al., 2000; Schmitz and Bowring, 2004; Griffin et al., 2005)

This composite craton is made up of the Kaapvaal and Zimbabwe cratons, separated by the high-grade Limpopo Belt. The *Zimbabwe Craton* contains a 3.5–2.8 Ga TTG complex, unconformably overlain by the 2.8–2.7 Ga Bulawayan Supergroup (komatiites, flood basalts, and sediments) and overprinted by ca. 2.6 Ga granitoids. The Great Dyke and its satellites cut the Craton at 2.57 Ga; during Proterozoic time the block remained uplifted, and no sedimentary basins formed.

The *Kaapvaal Craton* consists predominantly of granitoids with gneisses and narrow greenstone belts. Several terranes can be recognized on the basis of structural trends, the ages and distribution of greenstone belts, and granitoid ages, but much of the Craton is covered by Upper Archean basins, and terrane boundaries therefore are based on geophysical data. The *Southeastern Terrane* contains the oldest rocks, including 3.7–3.2 Ga gneisses, and the Mesoarchean Barberton greenstone belt experienced major 3.1–3.0 Ga magmatism. It is overlain by the 3.1–2.87 Ga Pongola Basin, the 3.07–2.7 Ga Witwatersrand Basin, and the 2.7–2.6 Ga Ventersdorf Basin. The *Central Terrane* is a narrow, NE-trending block consisting of 3.34–3.0 Ga gneisses, metamorphosed at ca. 2.6 Ga. The *Pietersburg Terrane* consists of 2.9–2.8 Ga TTG gneisses and greenstone belts, intruded by 2.7–2.6 Ga granitoids. The western parts of these three terranes are overlapped by 2.85–2.66 Ga supracrustal rocks, and then by 2.6–2.5 Ga Transvaal Basin rocks; the amalgamation of the eastern terranes occurred at >2.85 Ga. The *Western Terrane* is elongated N-S. It contains greenstone belts dated to 3.0–2.78 Ga on a basement of 3.25–2.88 Ga gneisses and granitoids. The 2.75 Ga granitoids occur on either side of the Colesburg Lineament, which marks the suture between the Western Terrane and those to the east. The northern part of the Craton was intruded by the 2.06–2.05 Ga Bushveld Igneous Complex.

The *Limpopo microcontinent* is an exotic crustal block caught between the Zimbabwe and Kaapvaal cratons, probably during a 2.7–2.6 Ga collision. It contains 3.3–3.1 Ga gneisses affected by granulite-facies metamorphism and granitoid magmatism at 2.7–2.57 Ga. The northern and southern marginal zones of the block are extensively deformed, and contain (possibly allochthonous) rocks correlative with the adjacent cratons. The peak of metamorphism was at ca. 2.56 Ga in the northern marginal zone, and at ca. 2.7 Ga in the southern zone. Metamorphism also may have affected the belt between 2.06 and 2.0 Ga, linked with events in the adjacent Kheis-Okwa-Magondi Belt, and the intrusion of the Bushveld complex.

Enigmatic Cratons (Proton/Archon? and Tecton/Proton/Archon?)

East Saharan Craton (also Sahara Metacraton and Ghost Craton)
(Schandelmeier et al., 1994; Abdelsalam et al., 2002, and references therein)

This mysterious block underlies much of the desert between the West African Mobile Zone and the Arabian-Nubian Shield. Exposed parts are dominantly medium-grade gneisses and migmatites, thought to be older rocks overprinted by Neoproterozoic tectonic events; rare Archean ages are recorded. Juvenile Neoproterozoic crust occurs along the eastern boundary. Pan-African granitoids (750–550 Ma) are widespread. Some studies suggest that the "East Saharan Craton" has been a single rigid block east of the Tuareg Shield, remobilized in Pan-African time. Alternatively, it may be a collage of terranes with diverse histories, swept together in late Neoproterozoic time.

Maltahohe Craton (Rehobothian Province)
(Anhaeusser, 1990; Hoal and Heaman, 1995; Ramokate et al., 2000; Becker and Branderbung, 2002; Kazmin, 2002; Hanson, 2003; Becker et al., 2004)

This is an enigmatic area between the Kheis-Okwa-Magondi Belt and the Neoproterozoic Damara orogenic system. An ancient craton (Maltahohe) may lie beneath Proterozoic rocks in the south-central part of the Province. The

1.79–1.73 Ga gneisses and migmatites, overlain by 1.25–1.1 Ga bimodal volcanics, crop out on the W and SW margins, and in tectonic windows to the N. The province was intruded by 1.4 Ga mafic-ultramafic rocks and 1.2 Ga granites; rhyolites erupted at ca. 1.1 Ga. Metamorphism of these rocks may have occurred only during the Pan-African Orogeny.

Mobile Zones

Areas immediately adjacent to (surrounding) the major cratons have been dominated by accretionary tectonics throughout the Proterozoic. These "mobile zones" include a variety of tectonic settings: Tecton, Proton, Tecton/Archon, Proton/Archon, and Tecton/Proton/Archon.

West African Mobile Zone (Black et al., 1994; Bruguier et al., 1994; Haddoum et al., 1994; Ferrié et al., 1996, 2002; Caby, 2003; Liègeois et al., 2003; Peucat et al., 2003)

The area east of the West African Craton contains several Archean to Proterozoic inliers, strongly affected by the Pan-African orogeny. The *Benin-Nigeria Shield* is a microcontinental block containing 3.7–2.9 Ga, TTG-type gneisses and deformed greenstone belts of Birimian age (2.2–2.0 Ga), intruded by 2.1–1.7 Ga and Pan-African granites. It docked with the passive margin of the West African Craton at 640–615 Ma, creating the Dahomeydes Belt of west-vergent nappes. The *Tuareg Shield*, comprising the Hoggar domains, includes Archean, Paleoproterozoic, and Neoproterozoic terranes, possibly amalgamated during the Eburnian Orogeny and intruded by 640–580 Ma Pan-African granites. Its Pan-African collision with the West African Craton is recorded in the strongly deformed Pharusian Belt, with ophiolites and arc-related volcanic rocks. The *Western Hoggar domain* includes Archean granulites and 2.65 Ga alkali granites, reworked during the Eburnian Orogeny (2.1–2.0 Ga). The *Central Hoggar domain* contains a thick stack of thrust sheets containing Archean complexes reworked in granulite facies in Eburnian time and overlain by ca. 2.2 Ga supracrustal rocks. Neoproterozoic subduction complexes are thrust onto the older rocks, and 620–580 Ma and 540–520 Ma granites are widespread. The *Eastern Hoggar domain* consists of migmatitic gneisses intruded by Pan-African granites.

Paleoproterozoic Fold Belts (Cahen et al., 1984; Hartnady et al., 1985; Lenoir et al., 1994; Möller et al., 1995; Maboko and Nakamura, 1996; Ring et al., 1997; Schlüter, 1999; Cornell et al., 1998; Feybesse et al., 1998; Boven et al., 1999; Muhongo et al., 2002; Ramokate et al., 2000; Tack et al., 2002; Hanson, 2003; Toteu et al., 2003; Cutten et al., 2004)

Several polycyclic mobile zones and single fold belts of Proterozoic age occur between and around the cratonic blocks of Africa. The *Ubendian Belt* extends for 800 km SW of the Tanzanian Craton; it consists mainly of metamorphosed supracrustal rocks from a continental passive margin environment. Especially in the SW part, these rocks have been subjected to high-grade metamorphism (2.03–1.97 Ga) and granitoid intrusion (1.93–1.86 Ga) during collision between the Tanzanian Craton and the Bangweulu Terrane. U-Pb geochronology and Hf isotope analysis of zircons (unpublished data courtesy of Albidon Limited) confirm that this orogen overlies Archean crust. The *Usagaran Belt* along the E margin of the Tanzanian Craton contains supracrustal rocks metamorphosed to granulite facies at 1.92–1.89 Ga, and 1.87–1.83 Ga calc-alkaline granitoids. Eclogites (ca. 2.0 Ga) occur in the central part of the Belt. The *Ruwenzori Belt* along the N edge of the Tanzanian Craton contains >2.0 Ga metasedimentary rocks of passive-margin affinity and tholeiites, folded and cut by 1.85 Ga granitoids, all thrust onto the gneisses of the Craton.

The composite *Kheis-Okwa-Magondi Belt* runs along the western boundary of the Kalahari Craton. In the thin-skinned, east-vergent *Kheis Belt*, 1.98 Ga basalts and clastic sediments rest unconformably on Archean basement. They were folded and metamorphosed at ca. 1.9 Ga, and intruded by granitic rocks at 1.27 Ga and 1.18 Ga, and by mafic dikes and sills at 1.12 Ga. The *Okwa Inlier* has a basement of ca. 2.1 Ga metamorphic rocks, which may be underlain by Archean rocks. The thin-skinned *Magondi Belt* NW of the Zimbabwe Craton contains a thick sequence of sediments and volcanic rocks deformed and metamorphosed at 2.1–1.96 Ga, and intruded by 2.0–1.93 Ga granitoids. The Kheis-Okwa-Magondi Belt was the Mesoproterozoic passive margin of the Kalahari Craton, and the extension of this margin is reflected in mafic and bimodal magmatism. Deformation of the Belt probably was caused by the accretion of terranes that today are buried beneath the Phanerozoic cover of the Nama Basin and the Neoproterozoic Damara Orogen.

The *West Central African Belt* evolved between 2.5 and 2.0 Ga along the western margin of the Congo Craton, and reflects the Eburnean collision between the Congo and Sao Francisco Cratons. It contains reworked Archean rocks, metamorphosed and intruded by 2.1–1.92 Ga granitoids, and is overlain by early Neoproterozoic rift-related sequences that may be connected with the breakup of Rodinia.

Mesoproterozoic Mobile Belts (Klerkx et al., 1987; Thomas et al., 1993; Jacobs and Thomas, 1994; Jacobs et al., 1997; Oliver et al., 1998; Robb et al., 1999; Dalziel et al., 2000; Goscombe et al., 2000; Frimmel et al., 2001; Mapani et al., 2001, 2004; De Waele and Mapani, 2002; De Waele et al., 2003; Hanson, 2003; Raith et al., 2003; Bulambo et al., 2004; De Waele and Fitzsimons, 2004; Duchesne et al., 2004; Johnson and Rivers, 2004; Kokonyangi et al., 2004, 2005; Tahon et al., 2004; Schmitz and Bowring, 2004; De Waele, 2005; Johnson et al., 2005)

The *Kibaran Belt* lies between the Congo and Tanzania cratons, and is thrust over the Paleoproterozoic Ruwenzori Belt. A Paleoproterozoic volcano-sedimentary sequence, deformed at 1.86–1.78 Ga, is exposed in the NE part of the Belt. Sediments from 1.4 Ga in age are intruded by 1.39–1.37 Ga S-type granites and large ca. 1.3 Ga mafic-ultramafic bodies. Tectonic rejuvenation at ca. 1.0 Ga produced more S-type granitoids. The *Irumide Belt* extends SW along the SE edge of the Tanzanian Craton and the Bangweulu Terrane. Archean and Paleoproterozoic rocks of the basement are overlain by 1.88 Ga rhyolites and sediments. The peak of metamorphism at 1 Ga was accompanied by widespread granitoid magmatism (1050–950 Ma). Farther to the SE, extensive areas of Mesoproterozoic gneisses have been called the *Southern Irumide Belt*, and interpreted as a stack of arc-related terranes imbricated during the Irumide orogeny. The *Choma-Kalomo Terrane* is a fragment of a Mesoproterozoic fold belt in southern Zambia; it contains 1.37 Ga granitic gneisses, and 1.2–1.17 Ga post-tectonic granites.

The *Namaqua-Natal Belt* wraps around the southern margin of the Kalahari Craton. Island arcs docked with the SW part of the Kaapvaal Craton at ca. 1.28 Ga. A 1.25–1.2 Ga volcanic belt developed on the Bushmanland microcontinent before its collision with the Craton around 1.2–1.1 Ga. In the western part of the Belt, rifting developed between 840 and 730 Ma, before a Pan-African (550–530 Ma) thermal event. This Belt is bounded to the south by the narrow Neoproterozoic-Paleozoic *Saldanian Fold Belt*.

Neoproterozoic Mobile Belts (Barr et al., 1984; Dallmeyer, 1989; Pin and Poidevin, 1987; Hanson et al., 1988; Pinna et al., 1993; Stern, 1994; Schwartz et al., 1996; Kröner et al., 1997, 2001; Hanson et al., 1998; Armstrong et al., 1999; Vinyu et al.,

1999; Kampunzu et al., 2000; Porada and Berhorst, 2000; Key et al., 2001; Mapani et al. 2001; Toteu et al., 2001; Kazmin, 2002; Ring et al., 2002; Thomas et al., 2002; Yibas et al., 2002; Hargrove et al., 2003; John et al., 2003; Katongo et al., 2004)

The basement of the *Zambezi Belt* contains Archean to Proterozoic gneisses, overlain by strongly deformed metasediments and granites. The Zambezi Basin developed by rifting at ca. 880 Ma; it was strongly deformed 870–820 Ma, and again during Pan-African time. The *Lufilian Arc* consists of deformed Archean to Proterozoic basement, overlain by Neoproterozoic volcanics and sediments, all thrust over the edge of the Congo Craton at 560–550 Ma. The *Damara Belt* is highly complex. In the Northern Zone, Neoarchean basement inliers and Paleoproterozoic lavas are overlain by ca. 750 Ma rift sequences, which pass upward into a thick turbidite sequence. The Axial Zone (Khomas Trough) contains turbidites, basalts, and alpine-type ultramafic bodies, representing an oceanic assemblage metamorphosed around 520 Ma. The thick sediments of the Southern Zone represent the passive margin of the block to the south, folded, metamorphosed, and thrust over the Belt from 690 to 485 Ma. The *Kaoko and Gariep belts* are the northern and southern coastal arms of the Damara Orogen, and consist of deformed rocks of the Neoproterozoic passive margins; their counterparts are found in coastal Uruguay and Brazil.

The *Oubanguides Belt* (Central African Fold Belt) occupies a wide band between north and central Africa. The 1.7–0.90 Ga sedimentary rocks overlie 2.0 Ga basement. Late Neoproterozoic charnockites and metasediments were thrust over the Congo Craton margin at ca. 565 Ma, accompanied by granitoid plutonism.

The *East African Orogenic Zone* represents a wide suture zone between East Gondwana and the various plates of West Gondwana. The *Arabian-Nubian Shield* is a collage of island-arc and backarc terranes, with remnants of 900 Ma and younger oceanic crust. Amalgamation took place from 800 to 620 Ma, followed by extension from 620 to 540 Ma, with the formation of gneiss domes, bimodal magmatism, and sedimentary basins. The *Mozambique Belt* extends from the Arabian-Nubian Shield along the east coast of Africa. The northern part contains both juvenile terranes and blocks of Archean to Mesoproterozoic continental crust, swept together from 800 to 500 Ma. Farther south, sediments of the early Neoproterozoic passive margin are tectonically intercalated with Archean gneisses in Kenya and Tanzania. The basement of southern Tanzania, most of Malawi, and northern Mozambique consists of Paleoproterozoic to Neoproterozoic gneisses, metamorphosed in Pan-African time.

A series of Neoproterozoic belts rings the West African Craton. The *Anti-Atlas Belt* is a typical foreland fold-thrust belt, developed by rifting, sedimentation, and volcanism along the Craton margin ca. 800 Ma, followed by northward-dipping subduction (750–600 Ma) to form an island arc that collided with the Craton at ca. 615 Ma. The *Trans-Saharan (Pharusian-Dahomeyan) Belt* is a zone of nappes along the eastern margin of the Craton; most deformation occurred between 650 and 550 Ma, during the collision between the Craton and the Tuareg and Benin-Nigeria blocks. The *Rokellides Belt* and the *Mauritanides-Bassarides Belt* run along the western side of the Craton; Neoproterozoic marine and continental clastics, and some rift-related volcanic rocks, overlie older basement and were deformed at 575–555 Ma.

The Pan-African tectonic episode ended with the amalgamation of Gondwana, which existed from Ordovician to middle Jurassic time. The Carboniferous Variscan Fold Belt along the NW edge of Africa marked the closing of the western Paleo-Tethys. Middle Jurassic time saw widespread Karoo magmatism in the southern part of the continent, preceding the breakup of Pangea and the formation of the modern oceans. During Cretaceous time a series of rifts with accompanied carbonatite magmatism cut Africa northeast from Benue; in Oligocene time the East African Rift began to form, leading to the opening of the Red Sea–Gulf of Aden in Miocene time. Cenozoic volcanism and associated uplift formed the Hoggar Swell in southern Algeria.

A TECTONOTHERMAL MAP OF THE UPPER LITHOSPHERE

The observations discussed above are summarized in a simplified map showing the tectonothermal age of upper lithospheric domains (crust and uppermost SCLM) across Africa (Fig. 2). The tectonothermal ages are assigned with reference to the crustal history. The boundaries of the domains have been defined using geological (including topographic), geophysical (gravity, magnetics, and seismic tomography; see below), and geochronological data. In areas of more detailed data, individual domains are typically 150–300 km across, but for the purposes of this map domains with similar histories have been clustered. *Archons* are shown where there is little evidence for major tectonothermal events after 2.5 Ga. *Protons* show areas of apparently juvenile crust 2.5–1.0 Ga in age, which has escaped later modification. *Tectons* show areas where juvenile crust has been generated at <1.0 Ga. Areas of Archean crust that have been reworked

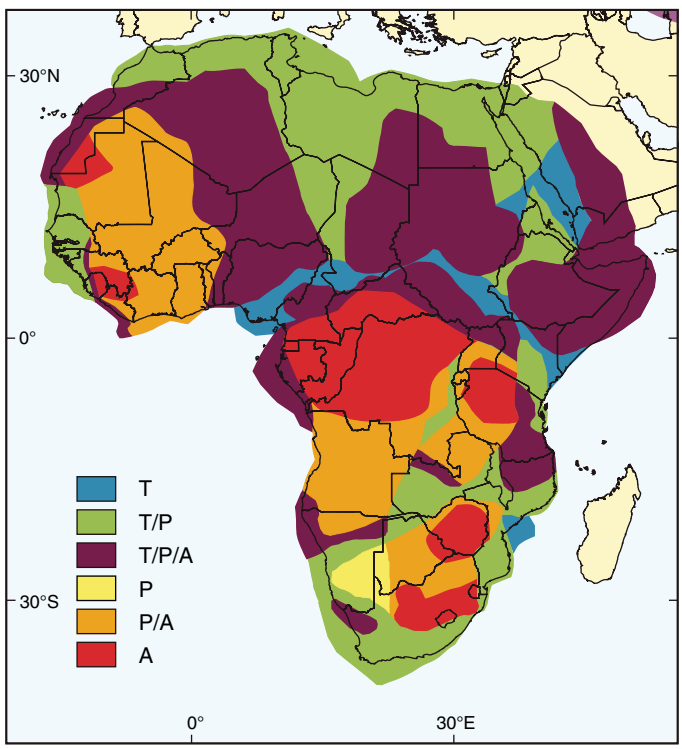

Figure 2. Map of the African upper lithosphere showing the tectonothermal age of different domains.

between 2.5 and 1.0 Ga are shown as Proton/Archon (P/A in Fig. 2); areas of Archean or Proterozoic crust that have been tectonothermally reworked since 1.0 Ga are designated Tecton/Archon (T/A) and Tecton/Proton (T/P), respectively. Areas labeled (T/P/A) are former Proton/Archon blocks reworked again since 1.0 Ga.

A key feature of the map is the extensive distribution of crust and upper lithosphere having an Archean heritage (A, P/A, T/P/A), including a large part of northeast Africa. A relatively modest proportion (ca. 30%) of African crust and uppermost SCLM is interpreted to be juvenile Proton (P and T/P), and much of this was reworked to varying degrees during Pan-African (ca. 650–500 Ma) time. Very little crust and upper SCLM appears to be juvenile Tecton, with the exception of parts of the Arabian-Nubian Shield and some of the rift zones across northern Africa. Significantly, many areas interpreted as juvenile Proton and Tecton (including Tecton/Proton) are covered by Neoproterozoic and/or Phanerozoic sedimentary cover sequences, and the possibility of an Archean substrate remains (e.g., much of northern Africa, the west coast of West Africa, southwest Zambia, and eastern Namibia). It is apparent that only portions of the Archean cratons have escaped reworking; the Congo Craton in particular has experienced crustal reworking around its edges, while the West African Craton is overlain by deformed cover rocks; the Proton/Archon classification assumes that this deformation has affected the basement as well.

SEISMIC TOMOGRAPHY

Tomographic Data

We use a shear (SH)-wave tomographic model derived from SH body-wave travel times following the approach of Grand (1994). The data include multi-bounce S waves and ScS waves. S and multi-bounce S waves that turn within the upper mantle are used to give better resolution of upper mantle structure than would be possible using only teleseismic shear-wave data. The velocity model is parameterized by blocks 75–150 km thick and 275 km on a side. As discussed by Grand (2002), lateral variations in seismic velocity are much larger near the surface than at greater depths. Therefore, we performed the tomographic inversion in steps with an initial inversion allowing only the upper 175 km of the mantle to vary in velocity and then proceeding to allow deeper heterogeneity. Variations in velocity are calculated relative to a starting model using a 1D reference structure for the mantle discussed by Grand (2002) and the 2D Crust 5.1 model of Mooney et al. (1998). The raw model is unsuitable for most display purposes, being constructed on an irregular 3D grid. It was thus interpolated using a modified 3D version of Shepard's method (Renka, 1988) and regridded to a 100-km cell size.

In most presentations of tomographic images, lateral velocity differences (from a predefined Earth model) are shown by a color spectrum in which high velocities are represented by "cool" colors (green to blue), and low velocities by "hot" colors (red to white). This practice reflects the interpretation of seismic velocities in terms of temperature, i.e., high temperatures produce low velocities. However, compositional variations in the SCLM account for at least 25% of the variation in S-wave velocity (Vs) shown in these images (Griffin et al., 1999; Poudjom Djomani et al., 2001; Deen et al., 2006), and these compositional variations are of major interest here. Therefore, in the images presented below, the traditional color scale has been reversed to simply reflect seismic velocity relative to the starting model; red to white colors denote high velocities, and dark green to blue colors show low velocities. This color scale also gives better definition of the heterogeneity within high-velocity regions.

The resolution of the model is limited by the original block size as well as available data. Checkerboard tests have been run for anomalies in each of the upper four layers. Figure 3 shows the results for a pattern of anomalies (2 × 2 blocks each) limited to the first layer (0- to 100-km depth; Fig. 3A), second layer (100- to 175-km depth; Fig. 3B), and third layer (175- to 250-km depth; Fig. 3C). The amplitudes of the input anomalies are not reproduced, but the lateral extents of the anomalies are well determined. Most of the error in the inversion is due to anomalies being spread in the vertical direction. This vertical smearing is evident in the immediately adjacent layers but weakens dramatically in successive layers. Smearing upward is more evident than smearing downward, and it is the latter that is of most concern here, given that the highest velocity anomalies occur in the top two layers. The checkerboard tests indicate that relative to the anomaly recovery in the input layers, downward smearing into the first layer below the input layer is reduced by a factor of 1.5–2, and into the second layer below the input layer by a factor of 3–4. This suggests that vertical resolution beneath anomalies is on the order of 100 km (most upper mantle layers in the model are 75 km thick).

Given that the 2 × 2 block anomalies in the checkerboard tests are close to the optimal lateral resolution of the model, a synthetic test was constructed to examine potential downward smearing associated with thick (150 km; top two layers), craton-sized, high-velocity lids in Africa. This test (Fig. 4) shows that the effects of these shallow anomalies are minor in the deeper layers (to 325 km), especially compared to the magnitude of the measured anomalies at 175–325 km. These test results indicate that the high-amplitude anomalies in layers 3 and 4 cannot be entirely due to smearing of anomalies from the overlying layers. Overall, the inversion should result in a good spatial mapping of average upper mantle shear velocity. In particular, although there may be some artificial smearing of shallow high velocity to greater depth, the inversion defines regions that have thick (at least 200 km) high-velocity lithosphere with good lateral resolution.

Major Features—Depth Slices

Figures 5–8 present horizontal slices through the tomographic model. The specific color scales chosen for individual layers have been chosen to reflect the overall decrease in ΔVs with depth, while enhancing our ability to image variability within a single layer.

Depth Slice of 0–100 km (Fig. 5)

In this depth slice, the cratons show up as red to white, indicating higher Vs, whereas the East Africa Rift shows as a dark-blue zone, denoting very low Vs. Areas of intermediate velocity (light green to yellow) extend westward across the Sudan, Chad, and Nigeria, and northward from the Hoggar Swell in southern Algeria. The East Saharan Craton (or Sahara Metacraton) is visible as a series of knobs with higher Vs. The high-Vs core of the West African Craton has relatively sharp, straight boundaries on the W, SW, S, SE, and NE sides, with several protrusions around the northern boundary. The center of the Craton, beneath the Taoudeni Basin, has subtly lower Vs than the immediately surrounding areas. The Congo Craton is seen as an ovoid block with weakly curved edges on the N, NW, SE, and NE sides; the W flank extends well out beneath the Atlantic, and the NW edge corresponds to the NE-SW Cameroon Line of volcanic islands. A large block with higher Vs lies offshore from the Namibia-Angola border. The Congo Craton is linked by a NW-SE belt of higher Vs to the Kalahari Craton, which consists of several centers of high Vs (Zimbabwe Craton and Kaapvaal Craton), separated by zones of slightly lower Vs. Part of the Tanzanian Craton is visible as a knob of low to intermediate Vs (green-yellow) on the S end of the East African Rift low-Vs zone. The Damara Orogen and the Namaqua-Natal Belt, like the Oubanguides Belt, are underlain by material of intermediate Vs with local higher Vs subdomains.

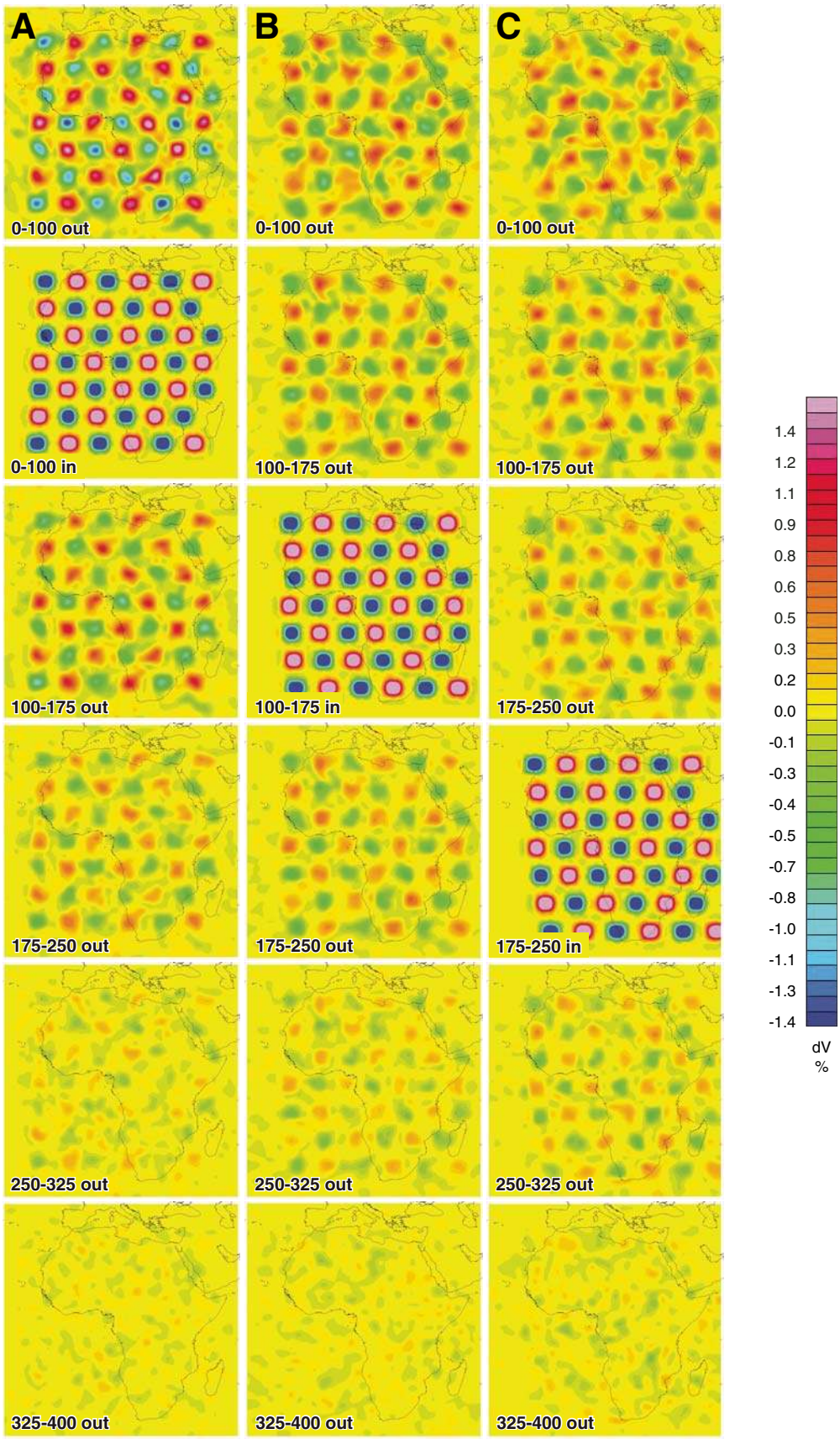

Figure 3. Checkerboard test of shear-wave tomographic model. Each column shows input anomalies introduced into a layer, together with output anomalies at layers 1–5 (0- to 400-km depth). A—anomalies introduced in Layer 1 (0–100 km); B—anomalies introduced in Layer 2 (100–175 km); C—anomalies introduced in Layer 3 (175–250 km).

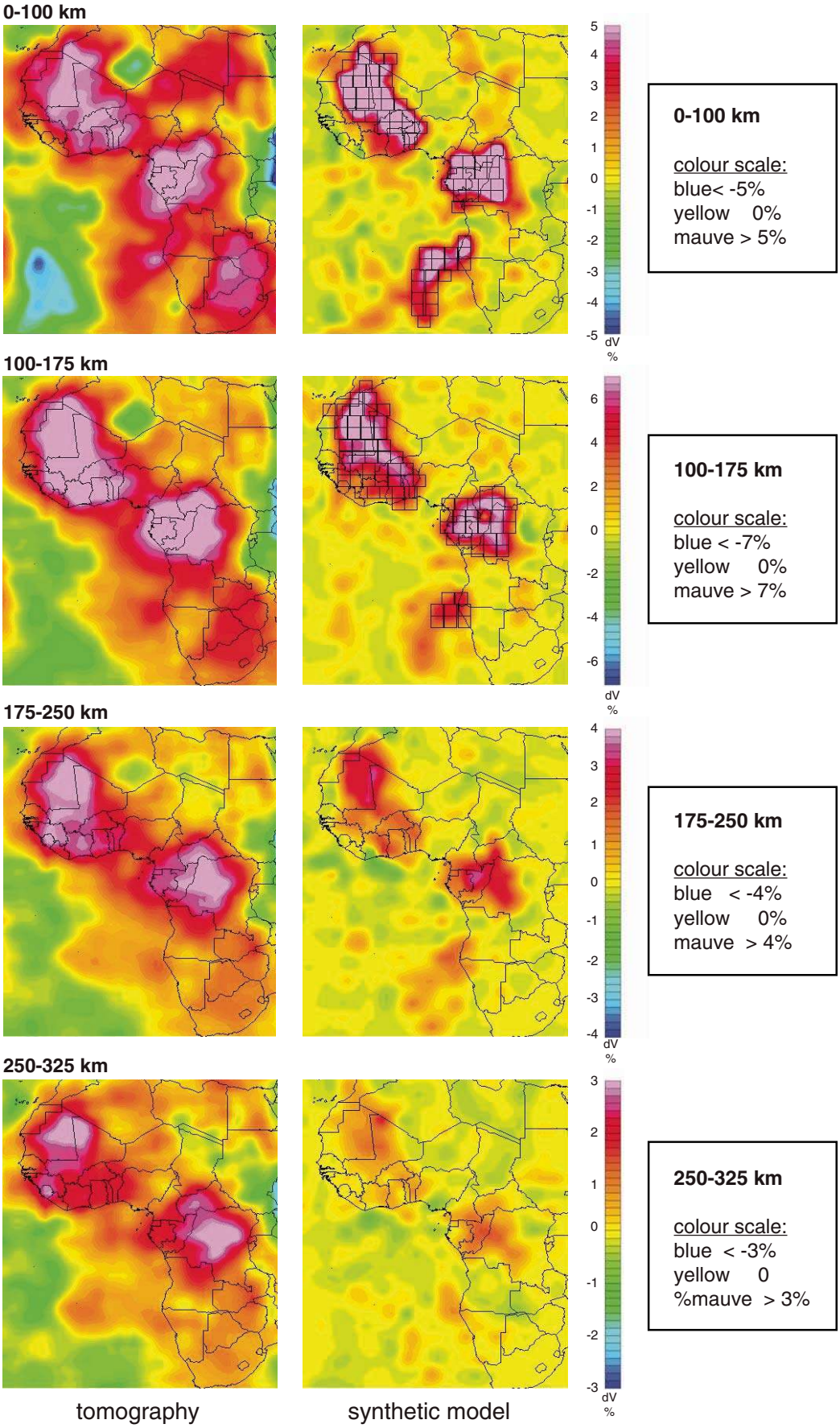

Figure 4. Test of depth smearing for a high-velocity lid of craton dimensions. Tomographic model in left column; recovered anomalies from synthetic model in right-hand column. Synthetic anomalies were introduced in Layers 1 and 2, as shown by box patterns in right-hand column. The results demonstrate that the observed anomalies at 250- to 325-km depths are unlikely to be produced by smearing from real anomalies in the upper two layers.

Depth Slice of 100–175 km (Fig. 6)

In this depth slice, the thermal effect of the East Africa Rift is similar to the overlying depth slice, but with a subtle expansion to the west. The Rift's low-Vs zone is bounded by a steep Vs gradient, especially toward the Congo Craton and the NE edge of the Arabian-Nubian Shield. As in the 0- to 100-km depth slice, lower-velocity zones also extend toward the west, around the northern boundary of the Congo Craton. The circular low-velocity feature beneath the Hoggar Swell is more pronounced in this depth slice.

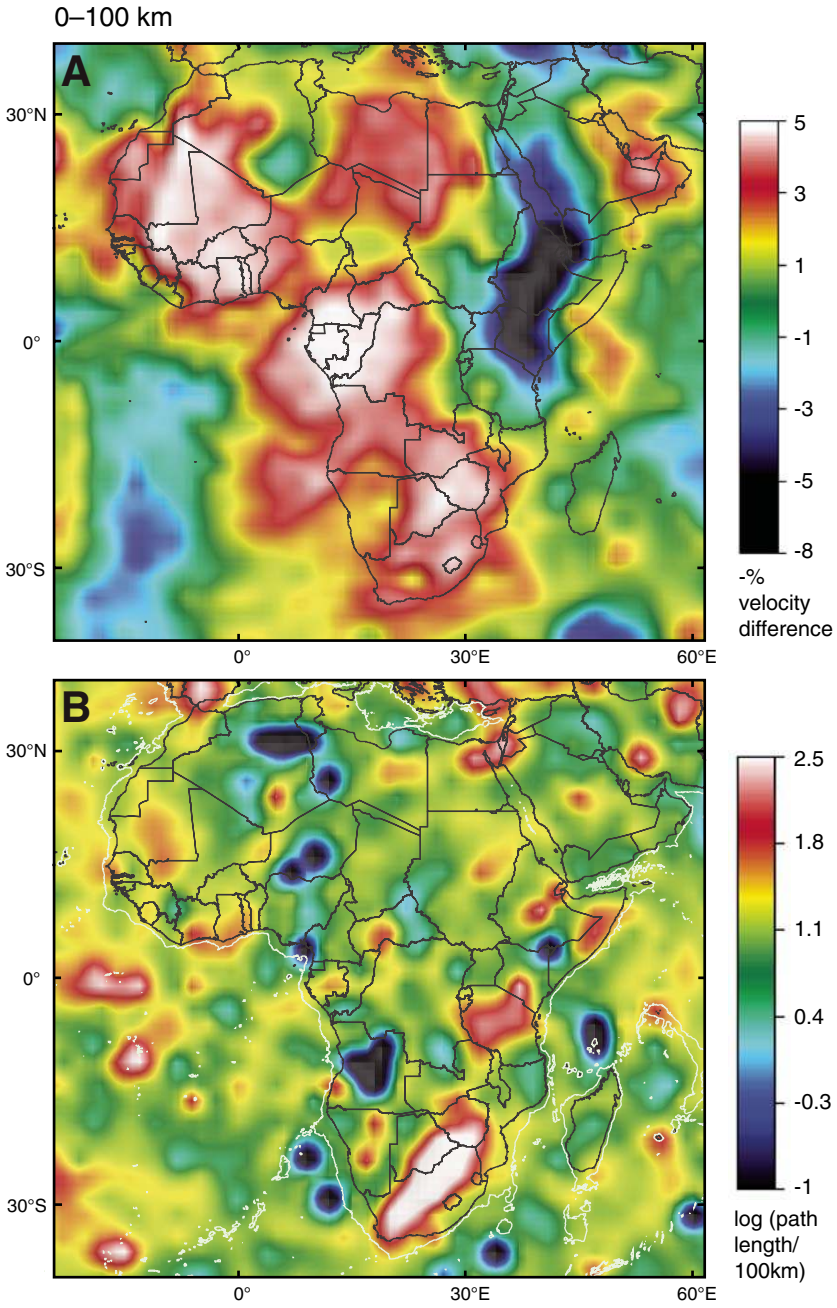

Figure 5. Upper panel shows tomographic image (S-wave velocity [Vs]) of Africa, 0- to 100-km depth slice; reference velocity is 4.6 km/sec. Red to white colors denote velocities much higher than the starting model; blue-green colors show Vs much lower than the starting model. Lower panel shows the density of ray paths through individual cells, expressed as log (path length/100 km). Areas with blue colors are poorly constrained, whereas yellow to white areas have relatively good ray-path coverage. White line outside the continental margins is the 2000 m bathymetric contour.

The West African and Congo Cratons stand out as large areas of higher Vs. The Kalahari Craton appears as several smaller knobs of moderately higher Vs, bounded by lower Vs along its margin in Botswana and the Namaqua-Natal Fold Belt. The mantle beneath the Bushveld intrusive complex has distinctly lower Vs than the areas immediately to the north and south. The edges of the two larger cratons, in particular, are largely defined by straight to weakly curved segments hundreds to thousands of km in length. Comparison with Figure 4 shows that these margins appear to be steep (i.e., their lateral migration with depth is limited), though this may be accentuated by the limitations of the tomographic model. One of these sharp boundaries, along the NW edge of the Congo Craton, extends well out beneath the Atlantic margin along the Cameroon Line of Quaternary volcanoes. The eastern and southeastern edges of the higher Vs area of the Congo Craton are sharp, but the SW portion of the Craton, which has been heavily reworked in Proterozoic time (Fig. 2) has lower Vs. However, the tomographic model is less reliable in this area. The relative Vs anomaly of the seaward extensions of the Congo Craton is less than in the 0- to 100-km depth slice. At the southern end of the East Africa Rift the Tanzanian Craton shows no higher Vs root in this depth slice, but the southern block of this Craton is recognizable as a small knob of slightly anomalous Vs surrounded by the low Vs of the surrounding Proterozoic mobile belts.

The Sahara Metacraton shows up as an irregular area of intermediate Vs, with considerable structure that is consistent with it comprising several terranes. Areas of higher Vs underlie parts of the West African Mobile Zone along the eastern side of the West Africa Craton. The accreted terranes of the East African Orogenic Zone are strongly affected by the thermal overprint of the East Africa Rift. The closed ocean of the Damara Orogen is underlain by intermediate Vs, similar to that beneath the Namaqua-Natal Belt.

Depth Slice of 175–250 km (Fig. 7)

In this depth slice, the thermal effect of the East African Rift is more concentrated toward the central part of the rift zone, but lower-velocity areas extending from it toward the W and NW are more pronounced and continuous. The low-Vs feature under the Hoggar Swell persists with depth and remains relatively stationary.

The West African Craton and the Congo Craton retain higher Vs "roots" at these depths, though with more range in amplitude. Their boundaries show only small displacements relative to their positions in the higher depth slices. The Kalahari Craton shows the largest changes with depth; in particular, the SW part of

the Kaapvaal Block shows low velocities compared to the other cratons. The expression of the southern block of the Tanzanian Craton is very weak in this layer.

At this depth the Sahara Metacraton appears to consist of several distinct blocks of intermediate Vs, with low-Vs zones between them. Similar material extends across Algeria N of the Hoggar low-Vs feature. The zone of higher Vs material off the coast of northern Namibia persists to these depths, and is separated from the Congo Craton by a belt of (mostly) low-Vs material that extends down into the Damara Orogen.

Depth Slice of 250–325 km (Fig. 8)

In this depth slice, much of northern Africa east of the West Africa Craton consists of low-Vs material, extending in several arms out from the East African Rift. At greater depths (not shown) these expand further, joining to form the top of the African Superswell (Nyblade and Robinson, 1994). The Hoggar feature remains stationary in this depth slice and below, suggesting that at least in the upper mantle, it represents a plume-like structure.

The northern part of the West African Craton persists as a high-Vs feature to these depths, with little change in its boundaries except for "erosion" along the northern edge. A belt of lower Vs separates this block from several higher Vs knobs along the S edge of the Craton. The Congo Craton also has a pronounced "root" at these depths, concentrated toward the SE part of the Craton; its eastern edge is defined by a sharp gradient toward the rift zone. The small root under the Zimbabwe Block has weakened, and at these depths the Kaapvaal Craton does not have a high-Vs signature. The higher Vs mantle seen offshore from the Congo Craton and the Angola coast is less pronounced in this depth slice, and the Damara Orogen has become a distinctly low-Vs zone. A zone of intermediate Vs links the low-Vs zone along the S margin of the Congo Craton to the East Africa Rift. The Sahara Metacraton has largely disappeared, and is visible only as remnants scattered among a series of low-Vs areas.

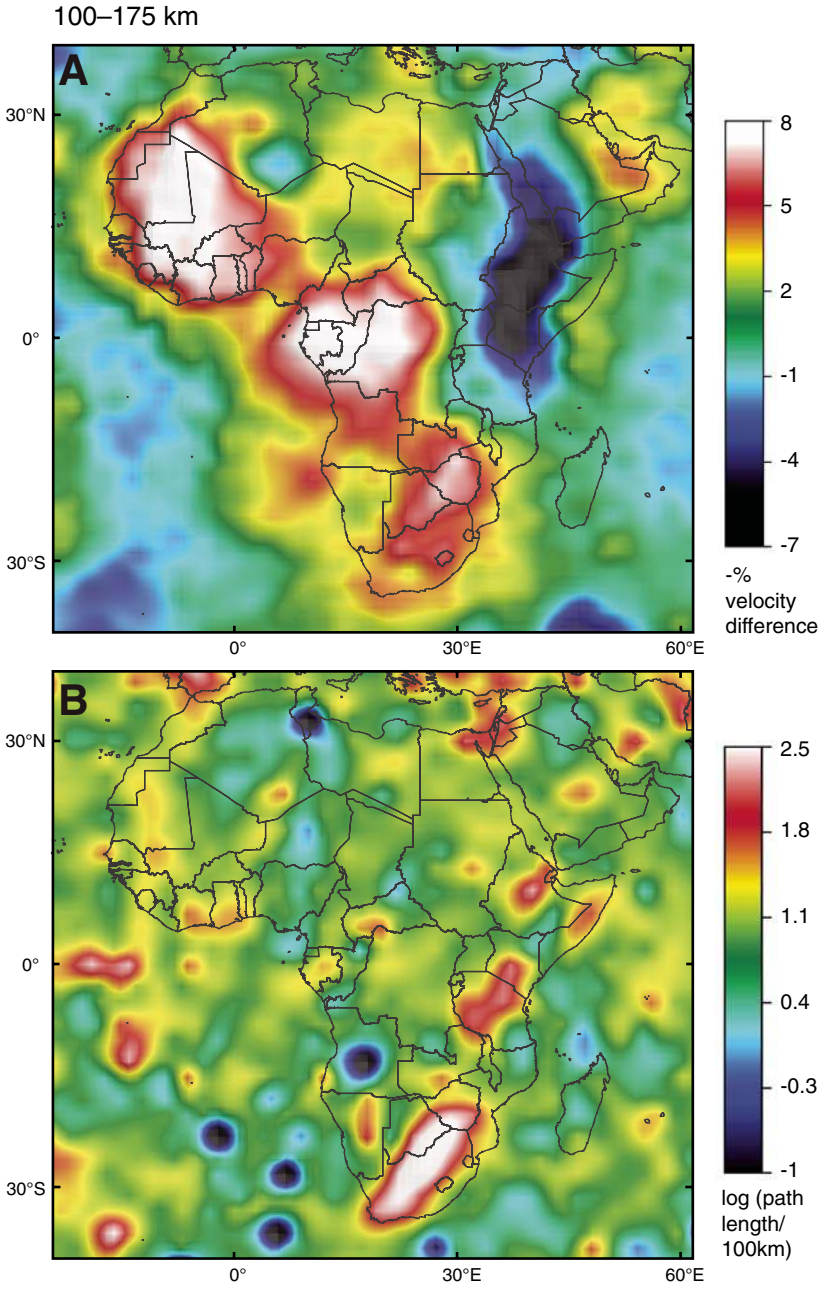

Figure 6. Tomographic image (S-wave velocity [Vs]) of Africa, 100- to 175-km depth slice, with map of ray-path coverage as per Figure 5. Reference velocity is 4.5 km/sec.

Tomographic Sections (Fig. 9)

A series of cross sections through the tomographic model to depths of 1000 km emphasizes the vertical and lateral heterogeneity in seismic velocity. Visualization of velocity anomalies over a significant depth range requires a normalization procedure, to ensure that the color scale or contours represent similar properties at each depth. Two materials in Layer 2 may have a given Vs contrast, but pressure effects will diminish this contrast, if the same materials occupy Layer 10. For example, Layer 10 in our model (850–1000 km) has a maximum Vs anomaly of 1.3% relative to the Earth model, whereas Layer 2 (100–175 km) has a maximum Vs anomaly of 8.4%. However, these two ranges may well represent similar variations in composition or temperature (T). A more robust representation can be produced by normalizing to the variance in the data, as all materials are subject to the same pressure effects. The sections shown in Figures 9 and 10 and the Animations therefore were constructed by first dividing the data in each layer by its standard deviation, and then linearly scaling the entire normalized data set so that the maximum and minimum values are the same as the original minimum (−8.8) and maximum (8.4) values in the un-normalized data (which occur in Layers 1 and 2, respectively). Physically, this is equivalent to moving each layer from depth to near-surface levels to calculate the Vs anomaly, and the resulting images should allow direct comparison of physically similar materials at different depths.

The most striking feature of Figure 9 is the extent and irregularity of the continental "roots." A series of higher Vs bodies (defined here by the transition from blue to dark green) is penetrated from below, and ultimately separated by narrow fingers of lower Vs material, which coalesce at greater depth (ca. 1500 km) to form the top of the African Superswell (Grand et al., 1997; Ritsema et al., 1999; Simmons et al., 2006, 2007).

In section AA′, the higher Vs root of the West African Craton extends to >300-km depth, especially on its east side. The root of the Arabian-Nubian Shield is similar in thickness, but markedly lower in mean velocity. The Sahara Metacraton has a thinner, lower-velocity root (ca. 150 km). The Hoggar feature (H) represents the top of a column of lower Vs mantle that extends to depths ≥1000 km. Despite their differences in Vs, the "roots" show sharp, steeply-dipping boundaries with the adjacent lower Vs mantle. In a section across the southern part of the West African Craton (BB′) the higher Vs root is ≥300 km thick.

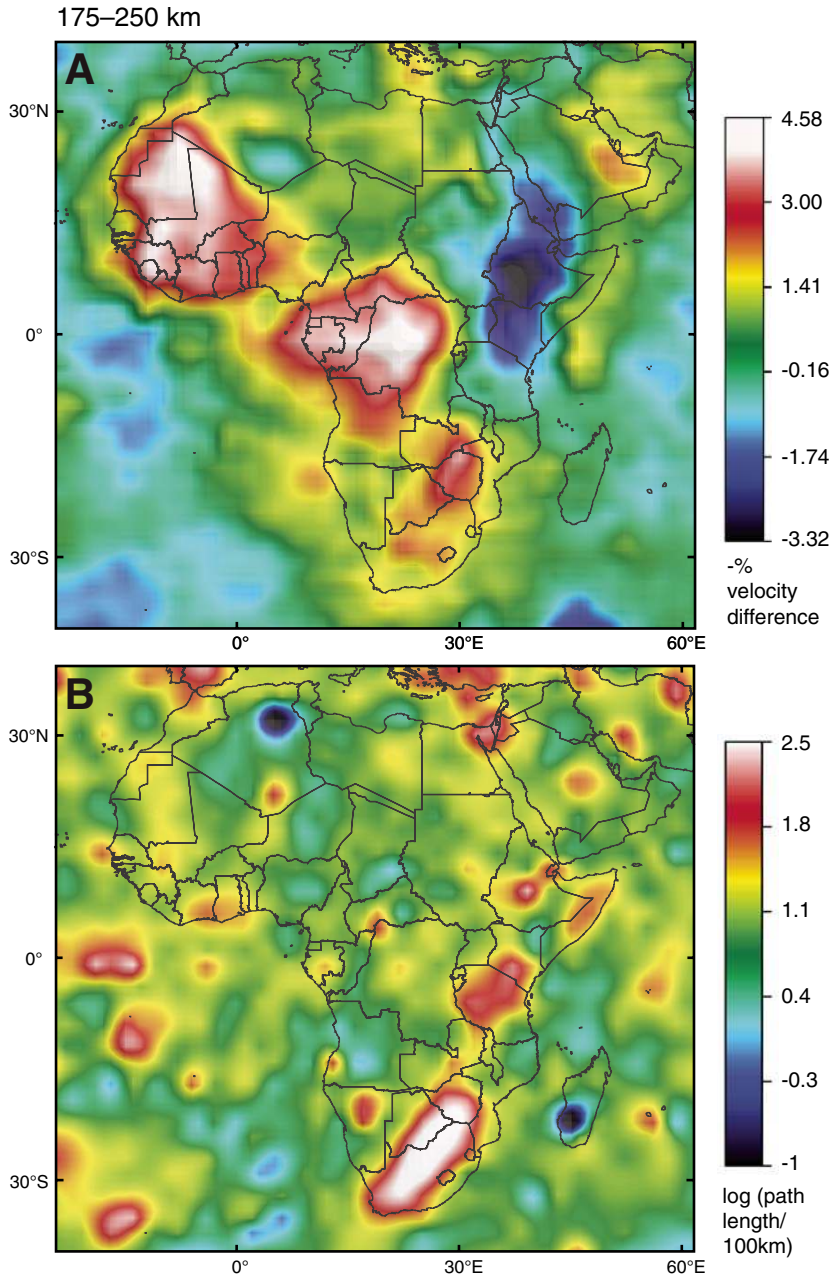

Figure 7. Tomographic image (S-wave velocity [Vs]) of Africa, 175- to 250-km depth slice, with map of ray-path coverage as per Figure 5. Reference velocity is 4.48 km/sec.

The lower Vs area extending westward from the East African Rift in the 100- to 175-km depth slice (Fig. 6) connects with the EAR. Section CC′ shows that the root of the Congo Craton extends to depths of 300–350 km adjacent to the EAR. This root extends at least 300 km out beneath the Atlantic Ocean at depths of 50–250 km.

Section DD′ extends from the western Atlantic Ocean, across the Kalahari Craton and Madagascar. It shows a wide band of higher Vs material to depths >100 km beneath the E margin of the Atlantic Basin adjacent to the Walvis Ridge, separated from the Kalahari Craton lithosphere by the lower Vs lithosphere beneath the Damara Orogen. Beneath the northern Kalahari Craton, higher Vs material extends to 200- to 300-km.

Section EE′ emphasizes the higher Vs and greater depth extent of the roots beneath the West African and Congo cratons, compared to the Kalahari Craton. The Benin-Nigeria Trough and the Damara Orogen separate these three cratons, and are characterized by thinner and lower Vs SCLM.

Section FF′, in contrast, emphasizes the deep extension of higher Vs material beneath the Congo Craton, the rising "fingers" of lower Vs material, and the apparent steep margins of both the Craton and the Arabian-Nubian Shield toward the East African Rift. The higher Vs root of the Congo Craton thins westward but extends >250 km seaward of the continental margin.

The transition from dark green to light blue that is evident in all sections is equivalent to an ~1.5% change in depth-normalized Vs anomaly; its origin is not clear. The variable depth at which this transition occurs, and its variable thickness, would seem to argue against this feature being an artifact of the data treatment or purely due to the vertical smearing implicit in the inversion and interpolation of the tomography model. It probably reflects variations in thermal or compositional gradients with adjacent mantle. Allowing up to 100 km vertical smearing, these sections imply that the base of the higher Vs parts of the roots varies between ~150 and 300 km, similar to global estimates of SCLM thickness (e.g., van der Lee and Nolet, 1997; Ritsema et al., 1999; Debayle and Kennett, 2000; Ritsema and van Heijst, 2000; Goes and van der Lee, 2002; Gung et al., 2003).

THREE-DIMENSIONAL MODEL (FIG. 10; ANIMATIONS 1 AND 2)

The tomographic data are presented in a 3D view, seen from below looking NE (roughly parallel to line F–F′ in Fig. 9); as in Figure 9, velocity anomalies have been normalized at each depth layer (equal standard deviations) for comparison. Volumes with depth-normalized

Vs ≥1.9% above the starting model are shown in red, and volumes with depth-normalized Vs ≥1.9% below the model are shown in blue. This image emphasizes the depth extent of volumes with mildly elevated Vs beneath the cratons, and the irregularity of their bases. The image in Animation 1 illustrates the effect of choosing different velocity-anomaly contours to define the roots; Animation 2 allows these volumes to be viewed from different azimuths. In light of the resolution tests on the tomographic model (e.g., Figs. 3 and 4), we regard the local extension of this higher Vs material to depths of >300 km as probably real, and comparable to the green to blue transition seen in the cross sections (Fig. 9). Given that the strongly depleted part of the SCLM is probably <250 km thick (see Mantle Petrology, below), the nature of these deep roots with mildly elevated Vs is not clear. However, they must reflect small differences in composition and/or temperature relative to the adjacent mantle. The relatively shallow root of high-Vs material beneath the Kalahari Craton, compared to the Congo and West African cratons, is striking. The low-Vs material along the East Africa Rift Zone and its subsidiary branches is interpreted as hot, relatively fertile "asthenospheric" mantle rising from the top of the African Superswell.

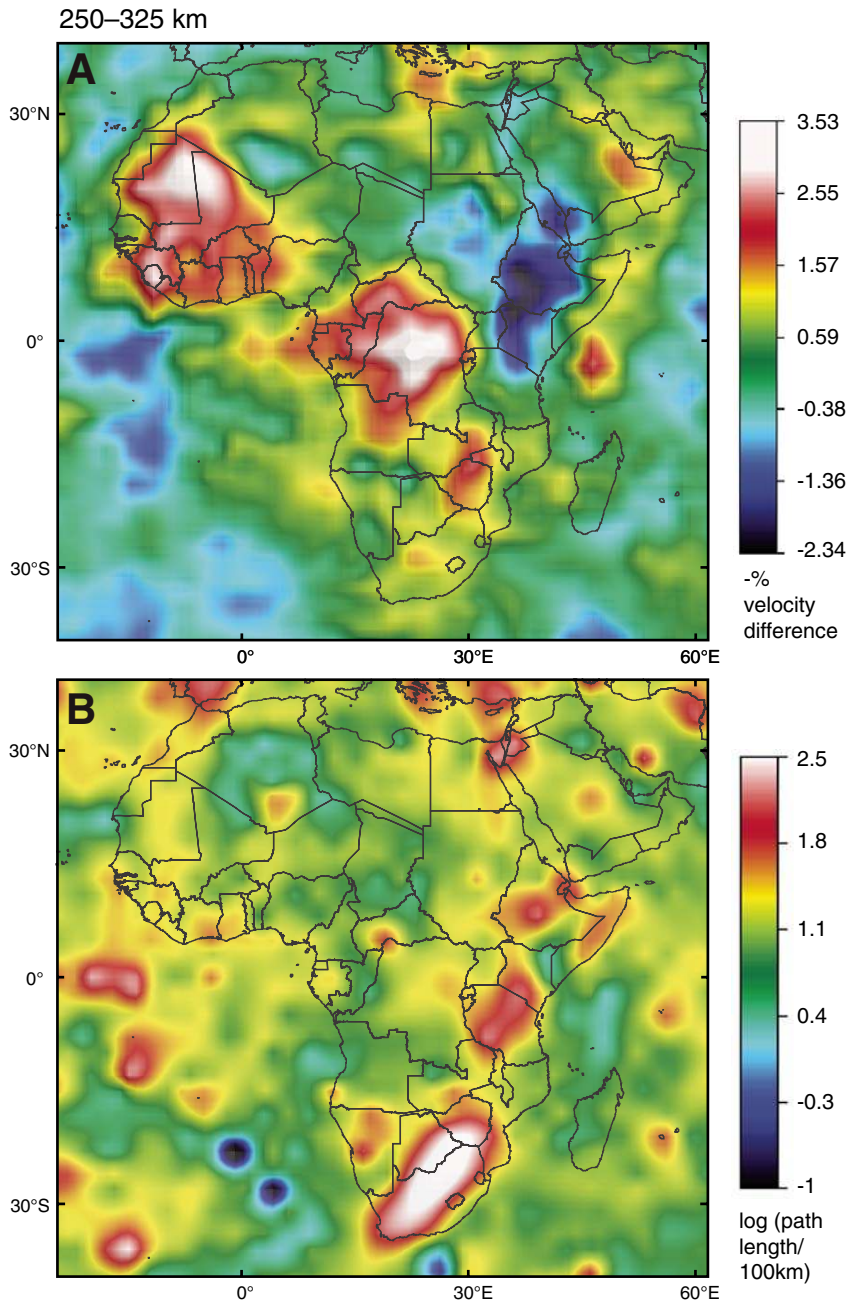

Figure 8. Tomographic image (S-wave velocity [Vs]) of Africa, 250- to 325-km depth slice, with map of ray-path coverage as per Figure 5. Reference velocity is 4.56 km/sec.

MANTLE PETROLOGY

Suites of mantle-derived xenoliths in volcanic rocks provide estimates of the geothermal gradient and composition of the subcontinental lithospheric mantle (SCLM) at the time of the volcanic eruption. The development of thermometry and barometry applied to xenocryst minerals in volcanic rocks has greatly expanded the number of localities for which such data can be obtained, and made it feasible to map the geology of the SCLM on a broader scale, both vertically and laterally (O'Reilly and Griffin, 1996, 2006). From garnet and chromite xenocrysts in kimberlites and basalts, we can derive profiles showing the variation with depth of mean olivine composition (a major control on seismic velocity), bulk-rock composition, density and calculated seismic velocities, as well as geotherm parameters and constraints on the thickness of the depleted SCLM. Such "Chemical Tomography" profiles (Fig. 11), coupled with Re-Os dating of peridotites and their enclosed sulfide minerals (Pearson et al., 2002; Griffin et al., 2002, 2004), indicate that Archean or Proterozoic SCLM is preserved, at least at shallow levels, beneath many areas of younger tectonothermal age.

The secular evolution in the composition of the SCLM (Griffin et al., 1999) is important for the interpretation of seismic tomography. Chemical tomography profiles indicate that Archon SCLM typically is strongly depleted in basaltic components; it is highly magnesian, thick (at least 160–250 km), and has low geotherms. Tecton SCLM is typically fertile (rich in basaltic components), Fe-rich, apparently thin (50–100 km), and has a range of high geotherms; the SCLM underlying Protons tends to be intermediate in these respects. The correlated variations in SCLM fertility, lithospheric thickness, and geotherm reinforce the effects of each on seismic velocity, and produce more rapid lateral variations in seismic response than would result from thermal effects alone. These correlations are the key to using seismic tomography images to map the lateral extent of different types of SCLM (Deen et al., 2006; O'Reilly and Griffin, 2006).

Chemical tomography sections for a number of localities across southern Africa can be used to illustrate the correlations between mantle type

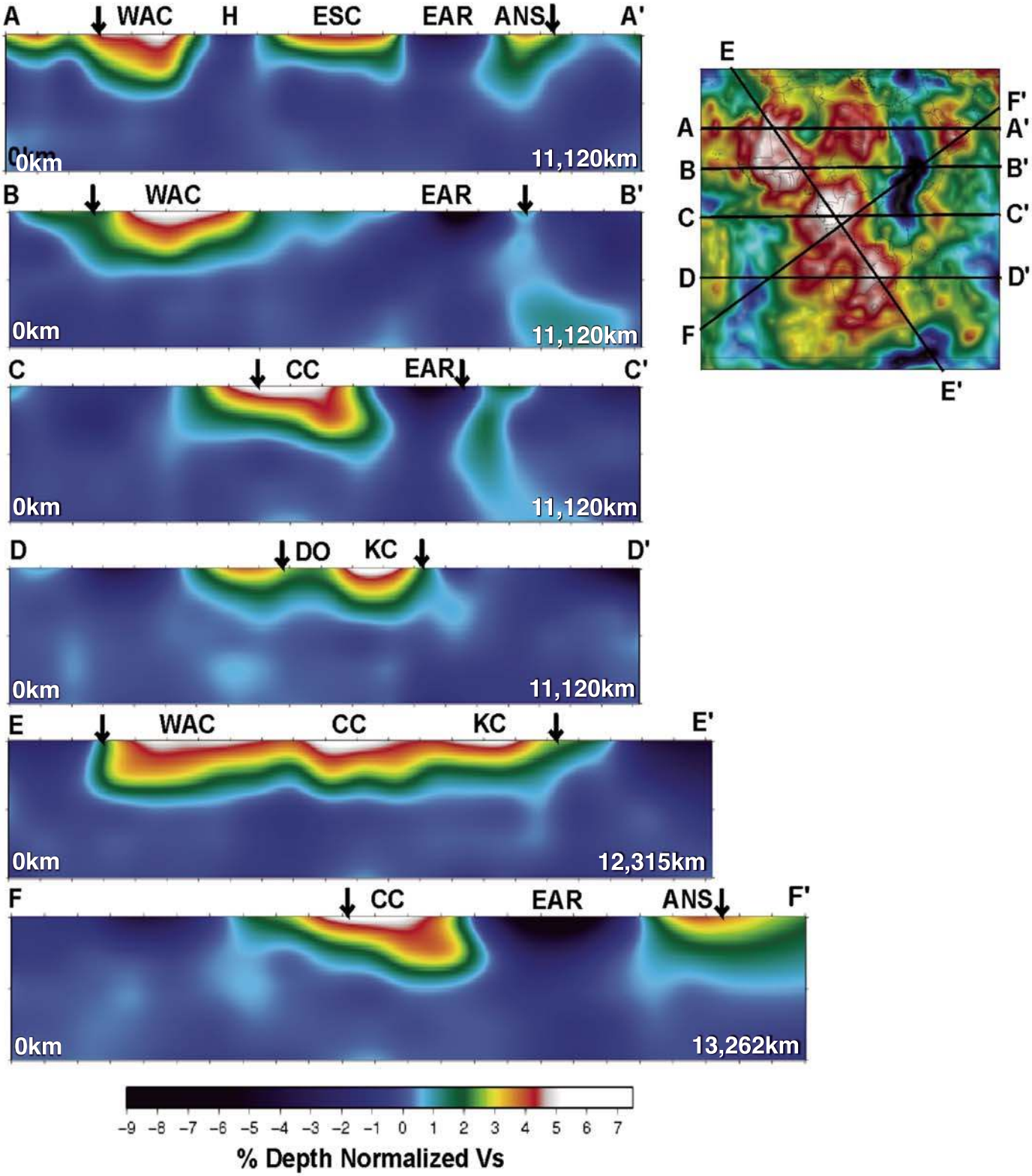

Figure 9. Cross sections through the upper 1000 km (10 layers) of the tomographic model, along lines shown in the map (0- to 100-km tomography from Fig. 4); no vertical exaggeration. See text for explanation of velocity scale. Vertical arrows on each section indicate the coastline. WAC—West Africa Craton; ESC—Eastern Saharan Craton; EAR—East Africa Rift; ANS—Arabian-Nubian Shield; CC—Congo Craton; DO—Damaran Orogen; KC—Kalahari Craton; H—Hoggar Swell; Vs—S-wave velocity.

and Vs, and to provide a basis for interpreting the seismic tomography images in terms of SCLM composition and history. An example is shown in Figure 11; vertical variations in rock types and degree of metasomatism are reflected in calculated Vs. Different styles of metasomatism have different effects on bulk composition and seismic velocity. Thus lherzolitic rocks produced dominantly by phlogopite-related metasomatism (green in Fig. 11) may still be relatively magnesian, whereas the melt-related metasomatism (red in Fig. 11) signature is typical of sheared lherozlite xenoliths, which have low Mg# and compositions approaching that of the convecting mantle, and hence lower Vs. The petrological data thus provide information on the vertical variation of Vs at a scale that rarely can be imaged by seismic techniques, but which can help to interpret the mean seismic velocities of individual areas.

Chemical tomography sections beneath Archean cratons typically show a depleted, variably metasomatized SCLM extending to depths of 150–250 km; the base of these sections commonly is marked by a zone of intense, melt-related metasomatism, which has been described as the "Lithosphere-Asthenosphere Boundary" (e.g., O'Reilly and Griffin, 2006; references therein). However, it is not clear that this term is appropriate, because there is no evidence from xenolith data, or from seismic data, that this melt-metasomatized zone is underlain by fertile, convecting mantle (i.e., the asthenosphere). Instead, it is possible that this "LAB" represents simply a level where mantle-derived melts have accumulated, metasomatizing the surrounding lithospheric mantle; this represents a minimum thickness for the depleted SCLM at the time of kimberlite eruption but does not constrain the maximum thickness of the SCLM (O'Reilly et al., 2008).

Data on paleogeotherms, derived from analyses of xenolith or xenocryst suites, are available from many kimberlites of different ages (500 Ma to <80 Ma) scattered across southern Africa. Kimberlite intrusion may represent minor thermal perturbations, but these would relax to an ambient geotherm within <100 Ma (O'Neill et al., 2005). The limited range of T recorded in xenolith geotherms (Fig. 12; c.f. Bell et al., 2004) suggests that present-day temperatures at depths of 100- to 175-km are relatively uniform within the cratons but higher in off-craton areas (Protons and Tectons). This implies that most of the variation in Vs *across the cratonic areas* is related to compositional variations (Deen et al., 2006). In general, highly depleted peridotites will yield high Vs, while more fertile compositions will give low Vs (Rudnick et al., 1998; Griffin et al., 1999; James et al., 2004; O'Reilly and Griffin, 2006). The Vs of the least depleted SCLM peridotites, which typically are found near the base of the depleted SCLM, approaches the Vs of the "asthenosphere" ("melt metasomatized" category in Fig. 11).

Comparisons between chemical tomography sections and the Vs tomography of the 100–175 km level are shown in Figure 13. More detailed tomographic imagery (P-wave velocity [Vp]) over part of this area by James et al. (2001) shows similar features (see below). The section sampled by the Group I (ca. 90 Ma) kimberlites of the SW Kaapvaal Craton (Fig. 11) is moderately depleted between 130 and 170 km but more fertile above ca. 130 km. The base of the depleted SCLM lies at 160–170 km, and fertility increases rapidly with depth toward the base of this depleted layer. This chemical variation produces strong vertical gradients in Vs but a moderately high mean value in this depth slice, reflected in the red to pink colors for this area in the tomographic model.

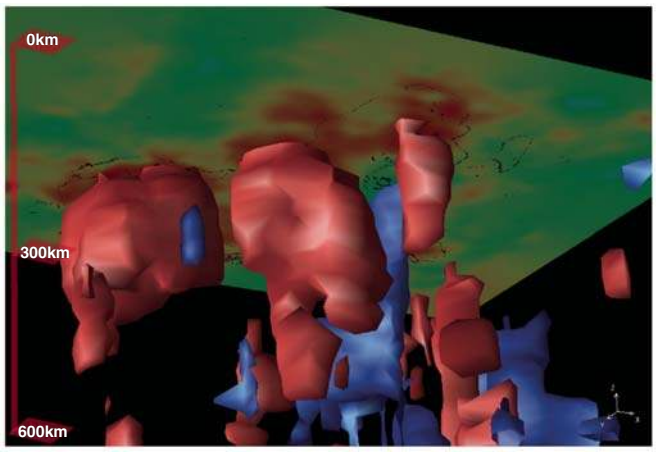

Figure 10. Three-dimensional representation of the tomographic model, looking up and to the NE from below the south Atlantic Ocean. Velocity anomalies have been normalized at each depth layer (equal standard deviations) for comparison. Red volumes have S-wave velocity (Vs) 1.9% above the normalized model; blue volumes have Vs 1.9% below the model. The higher Vs zones beneath the cratons are distinct from lower Vs (upwelling hot) material (East Africa Rift and offshoots) to depths >300 km. LAB—"Lithosphere-Asthenosphere Boundary."

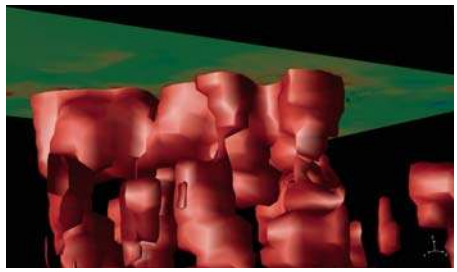

Animation 1. 3D representation of isocontours of positive-velocity anomalies beneath Africa (shaded red). African coastline and 0- to 100-km horizontal tomography slice plotted for reference. The anomalies are isocontoured between 1.2% and 2.4%, at intervals of 0.1%, and the results are presented as a time series. If you are viewing the PDF of this paper or reading it offline, please visit http://dx.doi.org/10.1130/GES00179.S1 or the full-text article on http://geosphere.gsapubs.org/ to view Animation 1.

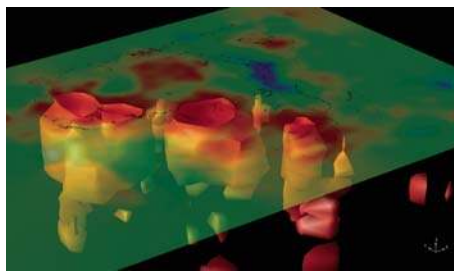

Animation 2. A perspective view of the depth-normalized, fast-velocity anomalies beneath Africa, isocontoured at +1.9%. The time series represents varying azimuth, viewed from the southwest. If you are viewing the PDF of this paper or reading it offline, please visit http://dx.doi.org/10.1130/GES00179.S2 or the full-text article on http://geosphere.gsapubs.org/ to view Animation 2.

The Limpopo Belt section is more strongly depleted and thicker; this would predict a higher Vs than for the Kaapvaal section. However, this area has only moderately high mean Vs (100–175 km); the discrepancy probably reflects reworking of the continental root by events subsequent to the 500 Ma intrusion of the kimberlites, including a major Karoo dike swarm (Griffin et al., 2003a). The kimberlites of northern Botswana (ca. 90 Ma) and southern Botswana (ca. 200 Ma) have sampled mantle sections that contain relatively little depleted harzburgite/lherzolite, and may reflect Proterozoic reworking of the Archean margin of the Kalahari Craton. The 1.2 Ga Premier kimberlite erupted through a mantle section affected by the 2.05 Ga intrusion of the Bushveld Complex. Xenolith suites contain abundant pyroxenites (Hoal, 2004), suggesting that the intrusion of mafic magmas refertilized the Archean SCLM in the 100- to 175-km depth range, and this is consistent with the relatively low Vs beneath this area (see also Fouch et al., 2004). The sections sampled by kimberlites near the boundary between the Kalahari Craton and the Namaqua-Natal Belt, and in the Kariba Valley (an area of Mesozoic rifting on the edge of the Zimbabwe Craton), appear to have thinner and more fertile SCLM than any of the more "cratonic" sections; they also have higher geotherms. These three factors reinforce one another to produce markedly lower Vs (yellow to pale-green colors) in the Namaqua-Natal Belt, and the transition to lower Vs on the NW edge of the Zimbabwe Craton.

The section from Tanzania is relatively depleted down to ca. 160 km, but deeper levels are strongly metasomatized, apparently by the intrusion of mafic melts (Griffin et al., 1994, 2003a; Chesley et al., 1999; Lee and Rudnick, 1999). The calculated mean Vs for the 100- to 175-km depth slice is comparable to that in northern Lesotho, while the green to blue colors beneath this area in the tomographic images show much lower Vs. This discrepancy clearly is related to the evolution of the East Africa Rift. The kimberlites used to construct the SCLM section and paleogeotherm are Cretaceous in age, and the observed low Vs is interpreted as reflecting the present-day thermal effect of the East Africa Rift. Surface-wave studies indicate that the depleted lithosphere beneath Tanzania probably is ca. 170 km thick (e.g., Ritsema and van Heijst, 2000; Weeraratne et al., 2003).

Alkali basalts scattered across northern Africa and along the East Africa Rift carry spinel-lherzolite xenoliths of fertile to moderately depleted compositions. Worldwide, such basalts are erupted along elevated advective geotherms similar to the well-defined southeast Australia xenolith geotherm (O'Reilly and Griffin, 1985; Xu et al., 2000), and typical SCLM thicknesses are <100 km, so that mean temperatures in the 100- to 175-km depth slice approach the mantle adiabat (1200–1300 °C). In our tomographic images, many of these localities are shown in yellow to green tones. However, localities in the East Africa Rift Zone, and the center of the Hoggar massif, have much lower Vs (blue tones in Fig. 6) in the 100- to 175-km depth slice. Deen et al. (2006) suggested that such low Vs could reflect the presence of fluids or melts in the 100- to 175-km depth range, consistent with the

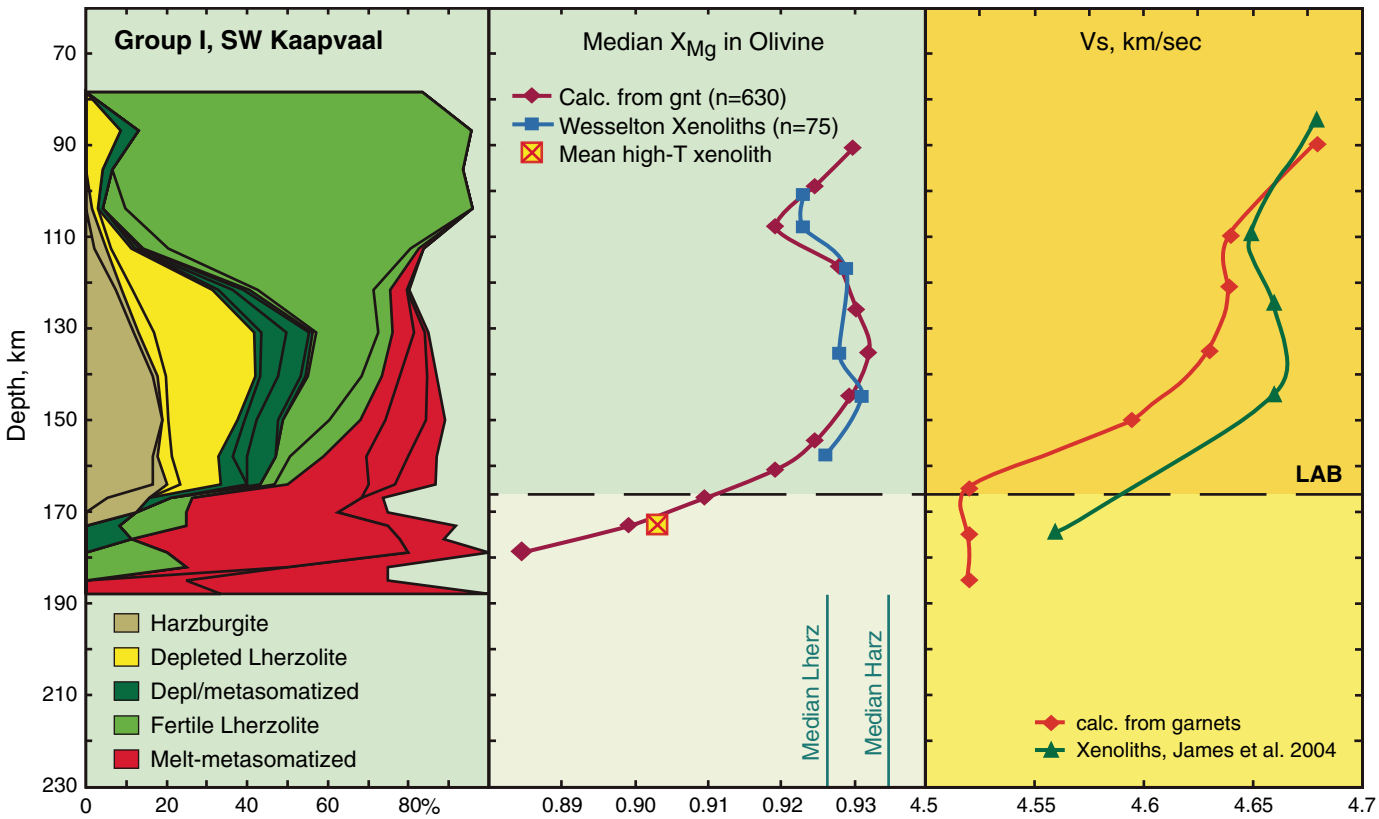

Figure 11. Chemical tomography section (after O'Reilly and Griffin, 2006) showing the vertical distribution of rock types and metasomatic signatures, the mean X_{Mg} of olivine, and the mean S-wave velocity (Vs) in a generalized subcontinental lithospheric mantle (SCLM) section sampled by the Group I (≤90 Ma) kimberlites of the SW Kaapvaal Craton. X_{Mg} is estimated from garnet-xenocryst compositions (Gaul et al., 2000); Vs is estimated by applying the algorithms of Hacker and Abers (2004) to whole-rock compositions and modes calculated from garnet xenocrysts as described by O'Reilly and Griffin (2006). Values of mean Vs calculated from xenoliths (James et al., 2004) are shown for comparison.

eruption of Neogene basaltic volcanoes. However, Afonso et al. (2008) have shown that the presence of melt is not required, because a similar effect will be caused by the high-T onset of anelastic attenuation in olivine.

In principle, there is no unique solution for the combination of SCLM composition and geotherm that will produce a given Vs. However, as noted above, there are strong worldwide correlations between SCLM composition, apparent thickness and geotherm, and a limited range of real geotherms and mantle compositions. Deen et al. (2006) examined the relationships between these factors and Vs, using a series of parameterized geotherms and the mean Archon, Proton, and Tecton SCLM compositions of Griffin et al. (1999). The results demonstrate that the high Vs represented by the red to white colors of Figures 6 and 13 can only be modeled using strongly depleted compositions and low conductive geotherms (30–35 mW/m^2). Areas such as the Sahara Metacraton, on the other hand, require more fertile compositions (≈Proton SCLM) and moderate geotherms, while areas such as the Damara Orogen were best modeled with Tecton compositions and moderate to high geotherms.

DISCUSSION

(1) Tectonic Evolution of Africa

The maps of crustal history and upper lithospheric domains (Figs. 1 and 2) can be used to reconstruct the tectonic evolution of the continent. The nuclei of Africa's great cratons (West Africa, Congo, and Kalahari) existed by early Neoarchean time (Fig. 14). Other fragments of Archean lithosphere were juxtaposed to these nuclei via a series of accretionary and collisional events throughout the Proterozoic. Here we briefly describe this series of events, with emphasis on periods of significant change. All directions and orientations are relative to present-day Earth coordinates.

(a) 2.7–2.5 Ga

The Archean cratons of West Africa, including greater Leo-Man-Ghana, Taoudeni, and Reguibat, probably were widely separated at this time. By ca. 2.8 Ga the core of the Congo Craton was ~2000 km across; on the southern edge the small Kasai Craton probably was accreted during Neoarchean time. The Zimbabwe Craton was amalgamated by a series of east-directed collisions between 2.68 Ga and the docking of the Limpopo microcontinent by ca. 2.60 Ga (Dirks and Jelsma, 2002). Collision of this combined Craton with the Kaapvaal Craton to form the Kalahari Craton occurred at either ca. 2.61 Ga (Griffin et al., 2005), or perhaps at ca. 2.0 Ga. The northern and southern Angolan Craton joined perhaps as early as ca. 2.64 Ga. Re-Os data on mantle peridotite xenoliths from the Kaapvaal Craton suggest that individual terranes carried their own SCLM roots into these collisions (Griffin et al., 2004). These events produced cratonic nuclei large enough to survive (at least in part) subsequent modification.

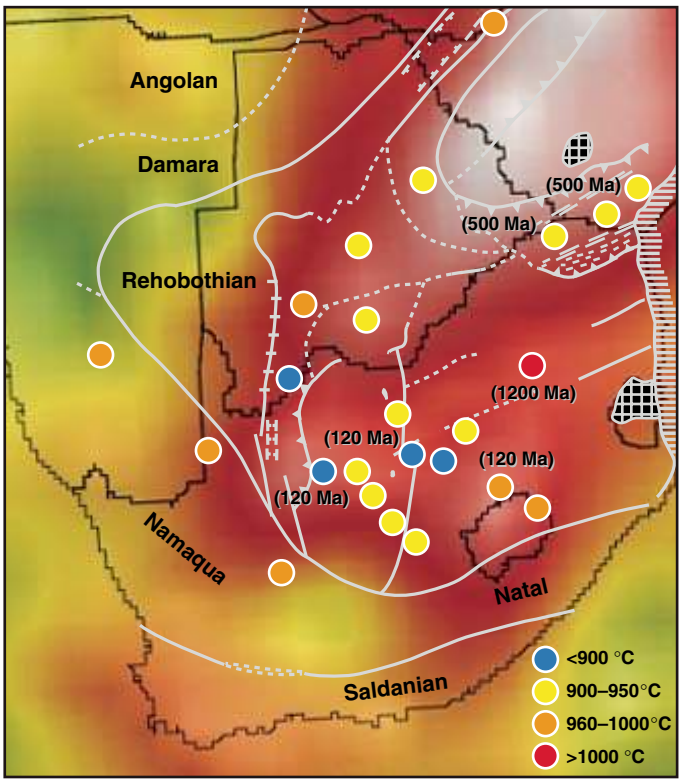

Figure 12. Map of southern Africa showing the distribution of temperature at 150-km depth, estimated from paleogeotherms defined by xenolith and xenocryst data on kimberlite pipes of different ages. Approximate ages of some kimberlites are shown in brackets; unlabeled ones were intruded at 85–100 Ma.

(b) 2.1–1.8 Ga

In West Africa, the Taoudeni Subcraton and Blocks to the west docked to Leo-Man-Ghana at ca. 2.1 Ga. The Okwa microcontinent probably accreted to the Kalahari Craton during the ca. 2.1 Ga Magondi Orogeny, followed by emplacement of the Bushveld Igneous Complex (2055 ± 4 Ma; Ramokate et al., 2000). The West Africa Craton collided with the Amazon Craton (not shown) along the Trans-Amazon Province to the SW at ca. 2.0 Ga (Santos et al., 2000, 2003). The Reguibat Craton also docked with West Africa at about this time, while the Congo Craton collided with both the Sao Francisco and Angola Cratons; the Gabon microcontinent was involved in this collision.

The Tanzania Craton collided with the Bangweulu domain at ca. 1.95 Ga along the Ubendian Orogen (Lenoir et al., 1994; Ring et al., 1997; Boven et al., 1999), followed by accretion of the Ugandan microcontinent in the north at ca. 1.85 Ga. This was followed at ca. 1.8 Ga by collision with the Congo Craton along the paleo–Kibaran Orogen, to form a coherent Congo-Tanzania-Bangweulu Craton. The Taureg Craton (formed by a ca. 2.0–1.9 Ga amalgamation of the Hoggar terranes) initially docked with West Africa at ca. 1.85 Ga. The timing of collision of the Maltahohe Craton along the western edge of the Kaapvaal Subcraton is poorly constrained; it is taken as ca. 1.9–1.8 Ga, though it may be as late as ca. 1.3–1.2 Ga (Eglington, 2006).

(c) 1.4–1.3 Ga

African Mesoproterozoic orogenic activity is limited to the margins of the Congo and Kalahari Cratons and the North Mozambique microcontinent. The latter behaved as a rigid block during Mesoproterozoic orogenesis. The sedimentary and magmatic record of the Kibaran Belt of the Congo Craton (Klerkx et al., 1987; Tack et al., 2002; Cutten et al., 2004) is consistent with a plume-related intracratonic rift setting (Tahon et al., 2004) that

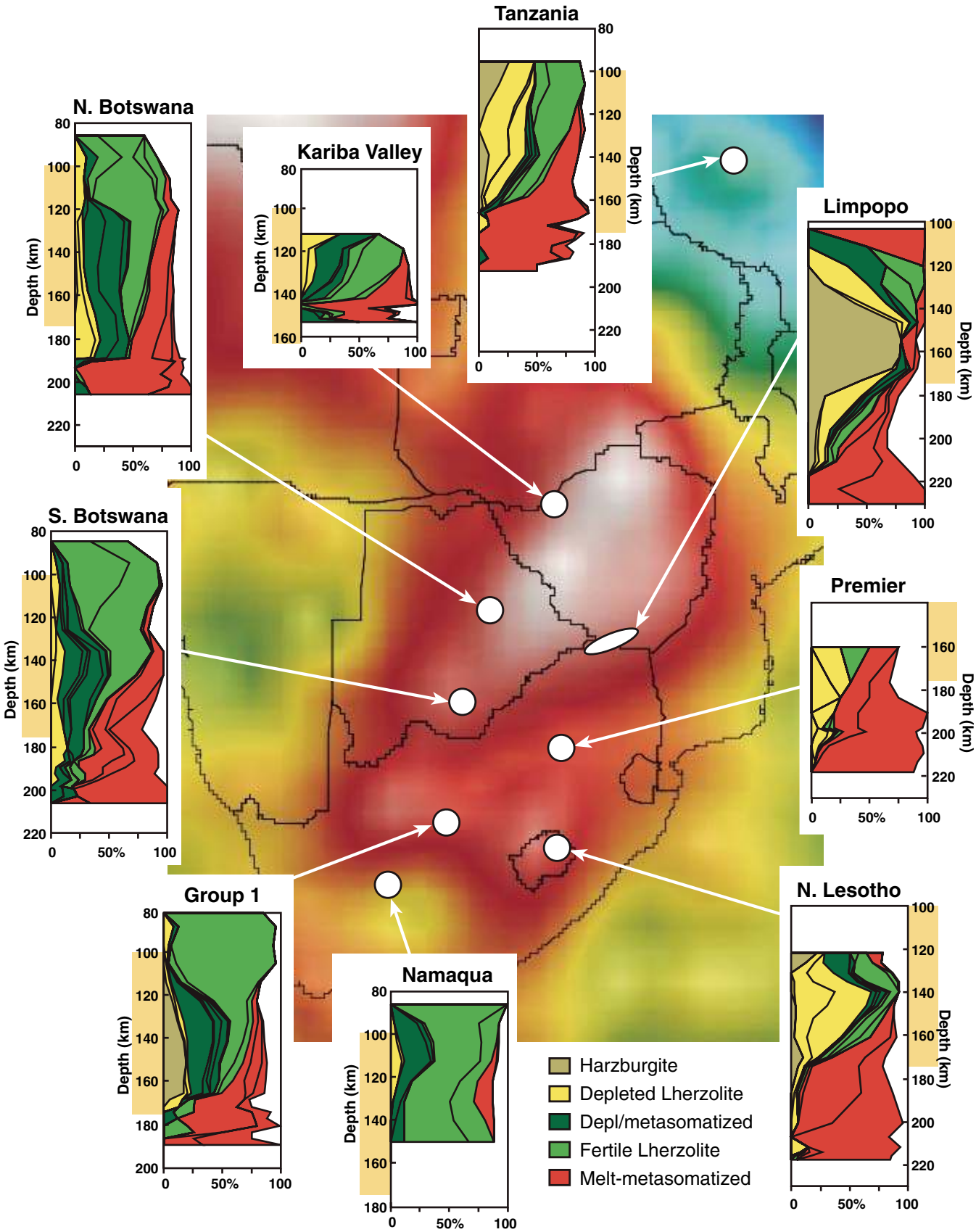

Figure 13. Chemical tomography sections for the subcontinental lithospheric mantle (SCLM) beneath selected kimberlite fields (after Griffin et al., 2003a), showing the relationships between SCLM composition and thickness and the seismic tomography model in the 100- to 175-km depth slice.

may or may not have generated oceanic crust. Accretionary events of this age are rare around the Congo Craton margin, and the continuity of any orogen to the south is obscured by Neoproterozoic sediments of the Lufilian arc. Arc activity occurred mostly to the south of the Kalahari Craton at this time (e.g., Namaqua Belt; Eglington, 2006), and the Choma-Kaloma Block in Zambia may have docked with the northwest edge of the Kalahari Craton at ca. 1.35 Ga or perhaps during the late Mesoproterozoic Irumide Orogeny.

(d) 1.2–1.0 Ga

The events of the Late Mesoproterozoic may be considered in a broad framework involving SSE-NNW convergence between the Kalahari and Congo-Tanzania-Bangweulu cratons, and the effect of stress transference across rigid cratonic lithosphere. A series of microcontinental belts (Sinclair zone, Gordonia, Namaqua, and southern Mozambique?) and island arcs (e.g., Tugela, Mzumbe, and Margate) accreted to the SW and SE edges of the Kalahari Craton from ca. 1.3–1.06 Ga (Eglington, 2006), possibly terminating with collision of the Saldania microcontinent. Convergence then switched to the northern margin of the Kalahari Craton, facilitating accretion of the Rushinga microcontinent (the basement to the Southern Irumide of Johnson et

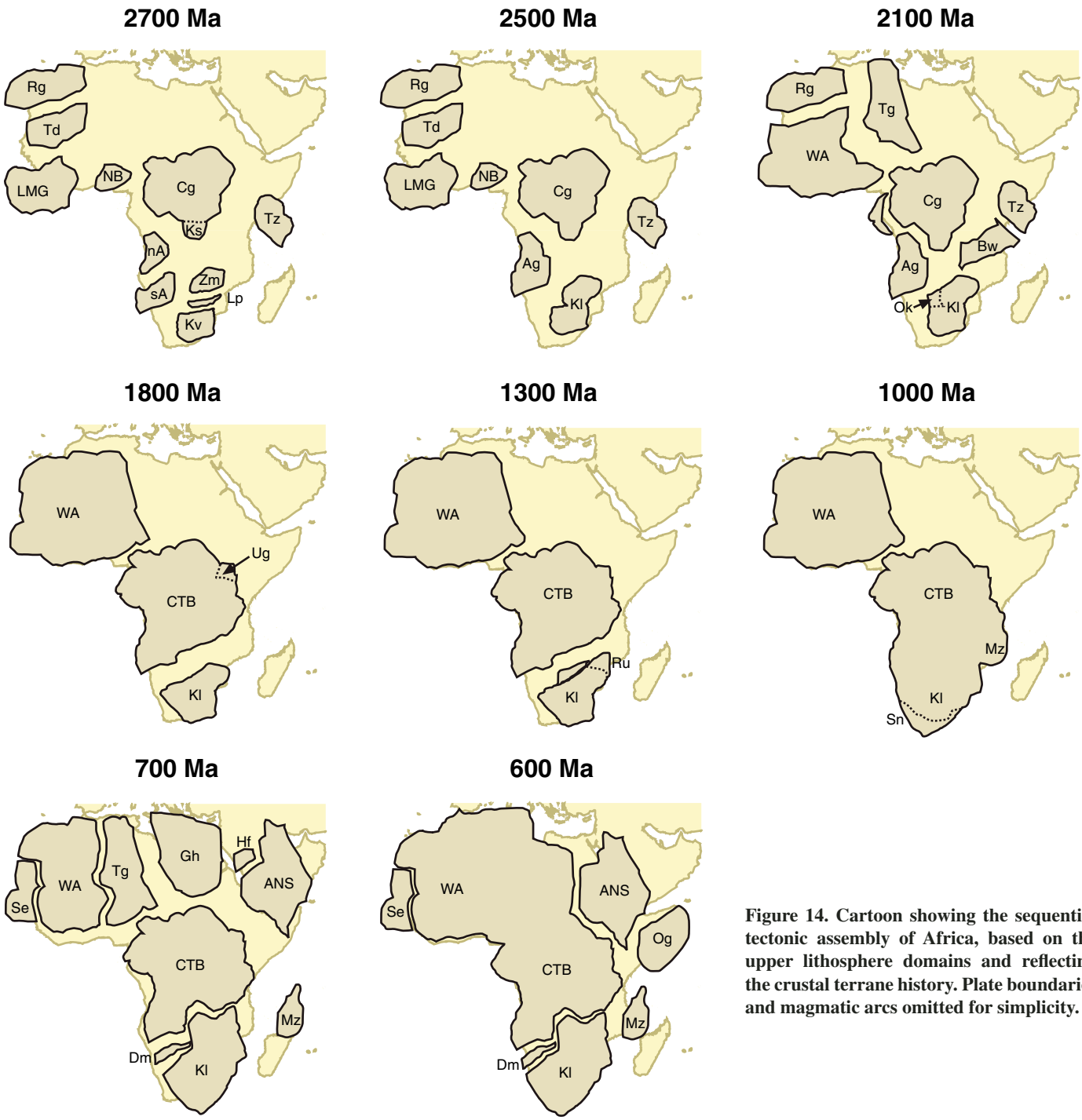

Figure 14. Cartoon showing the sequential tectonic assembly of Africa, based on the upper lithosphere domains and reflecting the crustal terrane history. Plate boundaries and magmatic arcs omitted for simplicity.

al., 2005) along the proto–Zambezi Orogen, and ending with collision along the Irumide Orogen at ca. 1.02 Ga (De Waele et al., 2003; DeWaele, 2005; Johnson et al., 2005). Movement on transcurrent faults in the Namaqua-Natal Belt persisted until ca. 980 Ma (Jacobs et al., 1997). The Mozambique microcontinent, created by amalgamation of a northern microcontinent with the Lurio microcontinent by ca. 1.05 Ga, may have been incorporated into the broader Irumide Orogen and accreted to a combined Kalahari–Congo-Tanzania-Bangweulu Craton at ca. 1 Ga (Pinna et al., 1993).

(e) 900–500 Ma

Rifting from ca. 800 Ma separated the Congo-Tanzania-Bangweulu, Kalahari, and Mozambique cratons; new oceanic crust may have separated the Kalahari and Mozambique cratons at this time. Early-Middle Neoproterozoic rifting of the Taureg Craton from West Africa created a marginal sea of undetermined width. The velocity response and apparent rigidity of a block of SCLM on the western margin of West Africa suggest the presence of a "Senegal Craton," which may originally have rifted off West Africa, or may be an exotic fragment that docked during the Pan-African Orogeny. The Eastern Saharan Craton probably was amalgamated from older fragments prior to the Neoproterozoic. The Arabian-Nubian Shield comprises a series of ca. 900–720 Ma island-arc terranes accreted to Archean microcontinents in the west and south at ca. 750–720 Ma.

Convergence and ocean closure during the Pan-African Orogeny began with collision of the Eastern Saharan and Taureg cratons at ca. 650 Ma, followed by collision with the West Africa Craton at ca. 620 Ma, forming the Pharusian-Dohomeyan Orogen, then with the Congo-Tanzania-Bangweulu Craton by ca. 600 Ma, forming the Oubanguides thrust belt. Later stages of the Pan-African convergence involved suturing of the Arabian-Nubian Shield to northern Africa, (re)docking of the Senegal Craton to West Africa, and final convergence and suturing of the Mozambique, Kalahari, and Congo-Tanzania-Bangweulu cratons. An (initially) low-angle collision between NW Kalahari and the Congo-Tanzania-Bangweulu Craton at 550–520 Ma (Johnson et al., 2005) formed the Damaran Orogen.

(2) Craton Margins, Rifts, and Continental Breakup

The summary above emphasizes the major role that the Archean cratonic nuclei have played in determining the tectonic history and structural fabric of Africa, and illustrates the importance of the craton margins as major discontinuities in composition and rheology. In the tomography, these margins appear as zones of strong gradients in Vs, extending to depths of ≥300 km around the West Africa, Congo, and northern Kalahari Craton. These steep gradients over considerable depth cannot be explained by temperature differences alone; they require large compositional gradients as well.

The very low Vs seen beneath the East Africa Rift and its branches across northern Africa could reflect the presence of fluids and melts (Deen et al., 2006) but can also be explained by the high-T anelastic attenuation of seismic waves in peridotite (Afonso et al., 2008). The tomographic sections (Figs. 9 and 10) suggest that the deep roots of the cratonic blocks play a major role in guiding the upwelling hot mantle emanating from the top of the African Superswell, in the upper few hundred kilometers of the mantle (c.f. Ebinger and Sleep, 1998; Sleep et al., 2002). The juxtaposition of this material with the cold, depleted cratonic roots produces the sharp Vs gradients at the craton margins.

The role of the craton margins in channeling fluids from sublithospheric depths is illustrated by the distribution of rocks produced by relatively low-degree melting, such as carbonatites, nepheline syenites, and kimberlites. These rocks typically occur in belts or linear arrays following the sharp Vs gradients around the cratons (Fig. 15). The edges of cratonic blocks are former tectonic sutures (e.g., the Proterozoic belts in Kenya, Uganda, and Tanzania; Burke et al., 2003), and these are prone to tectonic reactivation. Associated decompression melting, or small-scale convection generated along steep boundaries between lithosphere and asthenosphere (O'Neill et al., 2005), may explain the focusing of these low-degree melts along craton margins.

This control of deep lithospheric structure on magma emplacement is not confined to large-scale structures but extends to the smaller scales that can be resolved with regional seismic tomography. Figure 16 shows the distribution of kimberlites in southern Africa, superimposed on the detailed regional Vs model of Fouch et al. (2004). In this higher-resolution model, as in the global model, the kimberlites cluster around and between the high-Vs domains, or in low-Vs areas; they tend to avoid the high-Vs volumes, which are interpreted here as the least modified remnants of the original cratonic SCLM (Griffin et al., 2008).

The coincidence of the Cameroon Line of volcanoes with the NW edge of the Congo Craton

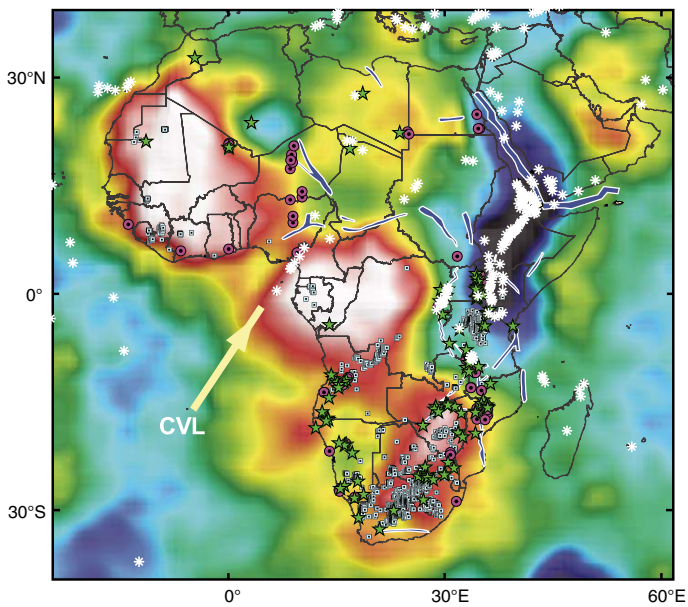

Figure 15. Distribution of low-volume melts (alkaline rocks, carbonatites, and kimberlites) and Mesozoic to Cenozoic rifts relative to the velocity structure and cratonic blocks (see Fig. 1) of Africa. Data on alkaline rocks and carbonatites from Woolley (1987); locations of kimberlites from Faure (2006). Blue polygons—rifts; white asterisks—volcanoes; green stars—carbonatites; pink circles—nepheline syenites; white squares—kimberlites; CVL—Cameroon Volcanic Line. S-wave velocity (Vs) image is 100- to 175-km depth slice.

(Fig. 15), including its offshore extension, is a striking example of the control of craton margins on magmatic activity. The last volcano at the SW end of the Line marks the NW corner of the seaward extension of the Congo Craton SCLM as seen in our seismic model. The Hoggar Swell, a major circular uplift >600 km in diameter and capped by Tertiary to Quaternary basaltic volcanoes, appears to lie above a narrow secondary "plume" rising from the African Superswell (Fig. 9, section AA′). Its position at the surface appears to be controlled by the margin of the West African Craton, and secondarily by major terrane boundaries within the Pan-African assemblage of northern Africa.

The passage of asthenosphere-derived magmas (particularly arc-, but also rift- and plume-related) and other fluids may be the major cause of modification of the cratonic SCLM, leading to a gradual and irreversible increase in fertility. However, the apparent craton-margin control of magmatism even where Vs is lower than in the craton cores suggests that modified cratonic SCLM can still retain its structural coherency. As a result, craton margins also have played a major role in localizing rifts (Fig. 15), and in the breakup of earlier continental assemblies (see above). This implies a large difference in lithospheric strength across the margins, consistent with the numerical modeling studies of Lenardic et al. (2000). The present trace of the East Africa Rift, and its branches across northern Africa, mostly reflect earlier sutures (e.g., Burke et al., 2003); Africa is once again being disrupted along ancient lithosphere-scale discontinuities.

(3) Cratonic SCLM—Composition, Origin, and Modification

The petrology of the Archean SCLM is known mainly from several well-studied xenolith suites, and estimates of its typical composition are based heavily on xenoliths from the Group 1 (≤90 Ma) kimberlites of the SW Kaapvaal Craton. However, comparison of chemical tomography sections from Group 1 and Group 2 (≥120 Ma) kimberlites (Griffin et al., 2003a) suggests that the SCLM underwent considerable modification between 120 and 90 Ma, and older sections such as that from the Limpopo Belt (Fig. 13) are considerably more depleted than younger sections from the rest of the Kaapvaal Craton. Thus the mantle sampled by the Group 1 kimberlites may not be representative of typical Archean SCLM. This supposition is strengthened by the tomography, which shows that the SW Kaapvaal Craton has a relatively low-Vs root, compared to the larger cratons (Figs. 6 and 9).

Figures 15 and 16 show that kimberlites tend to cluster around the peripheries of high-Vs areas (see also Jaques and Milligan, 2004; O'Neill et al., 2005), and thus have preferentially sampled more strongly modified (refertilized) SCLM. It would appear that no well-studied set of kimberlite-borne xenoliths from Africa has sampled the volumetrically dominant SCLM represented by the high-Vs cratonic roots. Integrated modeling of seismic, gravity, and topography data (Afonso et al., 2008) shows that these roots require an SCLM in which the upper parts (50–150 km) are dominated by strongly depleted harzburgite and dunite, similar to some xenoliths described by Bell et al. (2005). This composition may be a closer match to the "pristine" Archean SCLM than most published estimates (Griffin and O'Reilly, 2007; Griffin et al., 2008). The Vs tomography of Africa to 175 km (Figs. 5 and 6) suggests that this highly depleted material still dominates the cratonic roots beneath the West Africa, Congo, and Zimbabwe cratons, areas with very limited xenolith coverage (Fig. 15).

Our tectonic analysis indicates that most areas of Proterozoic tectonism and magmatism within Africa are concentrated along ancient craton margins, and their development has involved the modification of Archean crust which presumably was underlain by Archean SCLM (P/A and T/P/A in Fig. 2). Comparison of the tomography and limited xenocryst data suggests that the SCLM beneath most of these areas represents refertilized Archean SCLM, rather than juvenile Proterozoic SCLM. This suggestion is borne out by Archean Re-Os model ages on xenoliths from some Proton areas (P/A, Fig. 2; Carlson et al., 1999). One exception may be in southern Namibia, where xenoliths have yielded no Re-Os model ages older than the Paleoproterozoic (Carlson et al., 1999; Griffin, 2008, personal observ.).

The seismic velocity of Archean SCLM appears to show an inverse correlation with the number and duration of overprinting tectonothermal events. Such events include arc magmatism, arc accretion, cratonic collision, and intrusion of plume- or rift-related mafic mantle melts. Thus originally Archean terranes showing evidence

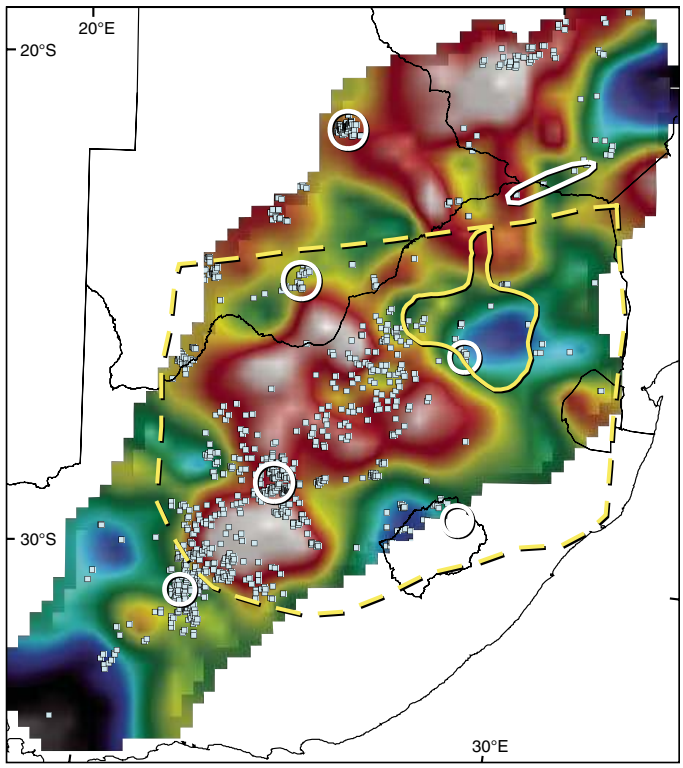

Figure 16. Detailed S-wave velocity (Vs) tomography model at 200-km depth across the Kalahari Craton of southern Africa (Fouch et al., 2004), with locations of kimberlites (Faure, 2006). Yellow dashed line outlines the Kaapvaal Craton; solid yellow line—Bushveld Complex. Circles and ovals mark locations of chemical tomography sections shown in Figure 13. At this level of detail, as well as on the regional scale (Fig. 15), the kimberlites cluster around the margins of high-Vs volumes and in low-velocity zones.

of repeated tectonothermal overprinting, such as the Sahara Metacraton, have lower velocity than less reworked Archean domains.

If correct, these observations would suggest that much of the secular evolution of SCLM composition from Archean through the Proterozoic described by Griffin et al. (1998, 1999), in fact represents modification of Archean SCLM, rather than the generation of juvenile intermediate-composition SCLM.

(4) A Tectonothermal Map of the SCLM (100–175 km)

Thermal-compositional modeling (Deen et al., 2006; Afonso et al., 2008), the correlations between xenolith and xenocryst data and seismic tomography (Fig. 13), and the map of crustal and upper mantle lithosphere tectonothermal history (Fig. 2) provide a basis for interpreting the seismic tomography in terms of SCLM composition and evolution.

Using the arguments presented above, we interpret the highest-Vs material in the cores of the major cratons (pink to white colors in Fig. 6) as consisting of highly depleted dunite and harzburgite, representing relatively unmodified Archon SCLM. The lower velocities around the high-Vs cratonic cores are interpreted as representing moderate refertilization of this original Archean SCLM by asthenosphere-derived melts and fluids, producing the garnet-lherzolite compositions commonly accepted as "typical Archean SCLM" (e.g., Griffin et al. 1999; Fig. 11). Further refertilization during subsequent tectonic events would produce still lower Vs, tending toward the velocities represented by green to yellow colors in Figure 6. If this mechanism is accepted, the map of tectonothermal domains (Fig. 2) can serve as a guide to the timing of the last major modification of the SCLM, and can identify domains in which the upper and lower lithosphere have been coupled, or decoupled, during major tectonic events.

Figure 17 shows an interpretation of the tectonothermal history of the 100- to 175-km depth slice (Fig. 6), which is the depth range best represented by xenolith data in southern Africa. Boundaries between domains are drawn on the basis of the tomography and available xenolith data; they are deliberately left "open" to emphasize the polycyclic and probably gradational nature of many boundaries. Comparison of Figure 17 with the upper lithosphere domains (Fig. 2) shows many similarities: most of the upper lithosphere Archons are underlain by unmodified Archon SCLM, and most Protons or Tectons are underlain by more fertile SCLM. These patterns are consistent with the concept of a strong coupling between the SCLM and the overlying crust. However, in a number of areas there appears to be a disjunct between the interpreted tectonothermal age of the upper and lower lithosphere, and these provide insights into tectonic processes.

In this interpretation, the West Africa Craton is largely underlain by Archon-type SCLM, although this block is shown largely as P/A in Figure 2. If correct, this implies that the Paleoproterozoic tectonic activity that affected much of the West African Craton did not strongly modify the Archean cratonic root. Mesoproterozoic to Neoproterozoic mobile belts along the eastern and western boundaries (Fig. 1) are underlain by less depleted mantle, interpreted here as refertilized Archon SCLM.

The Congo Craton is underlain mainly by Archon-type SCLM; on its southern margin, the survival of the high-Vs root beneath crust shown as P/A in Figure 2 reflects the relatively weak nature of the Proterozoic tectonothermal event in this area. Farther to the SW the Craton has much lower Vs at this level; limited xenocryst data show fertile garnet lherzolite compositions (V. Malkovets, 2007, personal commun.). We interpret these low velocities as showing that the SCLM has been strongly refertilized during the Proterozoic events (subduction, accretion, and collision) that have affected this area. Narrow zones of lower Vs along the eastern and northern boundaries of the Craton may also reflect modification of Archon SCLM during Paleoproterozoic and Mesoproterozoic (Kibaran) events on the eastern boundary and Paleoproterozoic and Neoproterozoic events on the northern margin.

The Kalahari Craton retains an irregular nucleus of Archon SCLM, strongly modified by Proterozoic tectonic events along its edges. The area underlain by the Bushveld Complex (central northern part of the Kaapvaal Craton), the related Molopo Farms Complex to the west, and the corridor between them, is distinctly lower in Vs (James et al., 2001; Fouch et al., 2004; Fig. 16), reflecting the severe modification of the SCLM seen in the Premier xenolith suite (Fig. 13; Danchin, 1979; Hoal, 2004). Low velocities along the southern margin of the Craton reflect both Mesoproterozoic and Neoproterozoic tectonic events.

The Tanzanian Craton (Fig. 1) is shown here as T/A; it contains Archon crust (Fig. 2), but the SCLM is overprinted by the thermal and metasomatic effects of the East Africa Rift (Fig. 13). The Lufulian Arc and the largely covered area to the SW are shown as T/P and T/P/A (Fig. 2) but are underlain by moderately

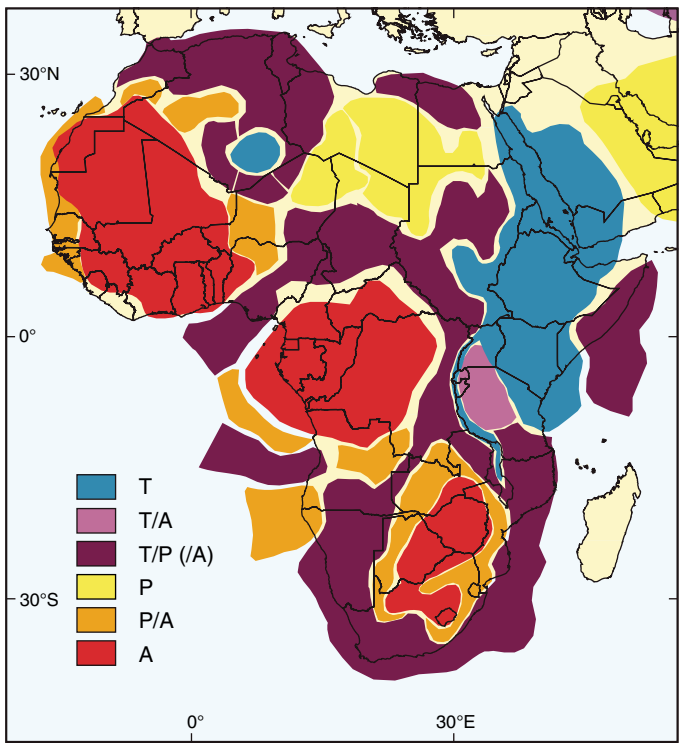

Figure 17. Interpretation of the seismic tomography model (100- to 175-km depth) in terms of the tectonothermal age of the subcontinental lithospheric mantle (SCLM). A—Archon; P—Proton; T—Tecton.

high-Vs mantle, interpreted here as modified Archon SCLM (P/A).

The relative paucity of juvenile Proton crust across Africa, despite a prolonged history of Proterozoic arc convergence, indicates that many of the Proterozoic terranes (including some island arcs) are built on fragments of older (Archean) SCLM, and that much of the juvenile Proterozoic lithosphere has been removed. Some preserved juvenile Proterozoic crustal terranes may be either allochthonous on modified Archean SCLM, or formed under dominantly extensional conditions, in which ascending melts experience little interaction with adjacent (older) lower crust.

Most of the SCLM beneath the Pan-African assemblage in eastern and northern Africa, including the Oubanguides Belt, is interpreted as originally Archean SCLM that has been strongly modified (refertilized) during Proterozoic and Pan-African tectonic activity. The Sahara Metacraton is clearly different to the other African cratons. Cryptic Archean crustal signatures among dominantly Proterozoic terranes suggest extreme tectonothermal reworking during multiple Proterozoic to early Paleozoic events (T/P and T/P/A; Fig. 2). It appears to have a relatively fertile "root," which may consist of several discrete blocks. These are interpreted (Fig. 17) as microcontinental blocks with strongly modified, dominantly Proterozoic SCLM, swept together during the Pan-African accretion event.

The SCLM beneath the East Africa Rift currently is being strongly thermally overprinted and metasomatized by fluids and melts related to Neogene volcanism, and hence is shown as Tecton SCLM; the same interpretation applies to the Hoggar low-Vs anomaly. Remnants of higher Vs material, which may represent small continental blocks with attached SCLM, occur in the Pan-African belt to the east and south of the Rift, including the offshore areas.

If Archean SCLM, albeit strongly modified, persists beneath many P/A areas, then the SCLM beneath many of the areas shown as T/P/A and T in Figure 17 may also represent reworked Archean SCLM. Indeed, the only juvenile "Tecton" SCLM beneath Africa may occur in the central part of the East Africa Rift, and its branches across northern Africa, including the Hoggar Swell. These interpretations remain to be tested by detailed Re-Os studies; they imply that the original volume of Archean lithosphere was much greater than presently mapped even by this study.

(5) Thickness of the SCLM

We have shown that apart from areas affected by high modern geotherms, there is a reasonable correlation between the composition of the SCLM as determined from mantle xenoliths and its seismic velocity response. The chemical tomography sections (Fig. 13) show that depleted SCLM extends from the base of the crust to depths of ~150 km below the Tanzanian Craton (Griffin et al., 1994, 2003a; Chesley et al., 1999; Lee and Rudnick, 1999) and ~200 km beneath parts of the Kalahari Craton. The geochemical methods are best suited to providing constraints on the *minimum* thickness of the depleted SCLM; the seismic data suggest that the continental roots extend, at least locally, well below the geochemically defined "LAB."

Although the heat of the East Africa Rift has reduced the Tanzania cratonic root to only a subtle feature in our body-wave SH model (Figs. 5–7), it is clearly visible to a depth of ~170 km in the surface-wave models of Ritsema and van Heijst (2000) and Weeraratne et al. (2003). Both of these models have depth resolution superior to ours. Significant parts of both the Congo and West Africa cratons extend to depths of >300 km (Figs. 9 and 10) in our body-wave SH model, compared to ~250 km in the surface-wave model of Ritsema and van Heijst (2000).

Within the Kalahari Craton our SH model shows elevated velocities extending to depths of 200–300 km beneath the Zimbabwe Craton, similar to the surface-wave model of Ritsema and van Heijst (2000; 200–250 km) and the body-wave model of Fouch et al. (2004; northern part of Fig. 16). Beneath the Kaapvaal Craton, our model shows a thinner, lower-amplitude, high-velocity root that fades rapidly with depth and is barely expressed in the 175–250 km layer (Fig. 7). This compares favorably with the chemical tomography sections (Fig. 13), in which the base of depleted SCLM varies from ~150 to ~200 km. Other studies of the Kaapvaal Craton indicate a root with minimum thickness of 150–200 km (surface-wave studies of Priestley et al. [2006] and Li and Burke [2006]), 200–250 km (e.g., body-wave study of Ritsema and van Heijst, 2000), 250–300 km (body-wave studies of James et al. [2001] and Fouch et al. [2004]; surface-wave study of Chevrot and Zhao [2007]), and ~300 km (receiver function study by Wittlinger and Farra [2007]). Surface-wave studies by Sebai et al. (2006) indicate thicknesses of up to 300 km for the West African, Congo, and Kalahari cratons.

(6) SCLM beneath the Ocean Basins

Along the west coast of Africa from Liberia to the Cape of Good Hope, the continental shelf is typically less than 100 km wide, as shown by the position of the 2000-m depth contour in Figure 5A. However, the tomography shows that the SCLM of the NW flank of the Congo Craton, for example, extends >300 km out under the Atlantic Basin (Figs. 5–7). In the area offshore from the Namibia-Angola border, another volume of high-Vs material, apparently detached from the main cratons, extends ca. 800 km out under the Basin at depths of 100–175 km (Figs. 5–7 and 9, section DD′).

The NW edge of the Congo Craton appears to control the distribution of the Cameroon Line volcanoes (Figs. 5–7 and 9, section CC′; Fig. 15). A traverse SE toward the Gabon coast from the offshore Cameroon Volcanic Line reveals a narrow zone of oceanic crust, then a 100-km-wide, NE-SW–trending zone of proto-oceanic crust (Meyers et al., 1996) also known as the Kribi Fracture Zone (see Lawrence et al., 2002), followed by a 100- to 200-km-wide offshore zone of rifted continental (pre-Atlantic) crust belonging to the North Gabon Rifted Terrane (Lawrence et al., 2002; Huismans and Beaumont, 2008). No oceanic crust is known over the bulk of the tomographic feature, consistent with the absence of ocean-floor magnetic striping (Korhonen et al., 2007). Onshore and offshore alkali basalts from the Cameroon Volcanic Line are geochemically and isotopically indistinguishable (Fitton and Dunlop, 1985; Lee et al., 1994; Ballentine et al., 1997); their high-μ (HIMU) signature may reflect interaction with metasomatized continental lithosphere.

The presence of these remnants of continental lithospheric mantle beneath the Atlantic Basin suggests that the opening of the ocean involved thinning and listric detachment of continental crust from its underlying mantle (perhaps with part of the upper SCLM), rather than a vertical alignment of SCLM and crustal fractures. Recent seismic studies in the western Atlantic SE of Newfoundland (Van Avendonk et al., 2005) have identified a 120-km-wide zone of thinned continental crust that appears to have detached from its underlying SCLM during opening of the Atlantic. On the corresponding eastern Atlantic margin offshore from the Iberian peninsula, SCLM without overlying continental crust is exposed in a zone ca. 100 km wide (Pickup et al., 1996; Dean et al., 2000; Shillington et al., 2004). This situation is analogous to the evolution of the Tethyan Basin, as preserved in the ophiolites of the Ligurian Alps. Detailed studies (Rampone, 2004; Rampone et al., 2005) indicate that the continental SCLM was unroofed during the opening of the ocean; this SCLM was then intruded by basalts, and covered by younger supracrustal sequences, before finally being exhumed during nappe emplacement as the ocean closed again. A similar situation has been described from Finland (Joruma ophiolite; Peltonen et al., 2003) where

the Archean SCLM was unroofed during the opening of the Svecofennian ocean and became the basement for deposition of a Svecofennian oceanic supracrustal sequence.

Despite the thermal effects of oceanic magmatism, the tomography suggests the existence of numerous small volumes of higher Vs material scattered through the Atlantic Basin. One such volume, beneath part of the Cape Verde islands, has been shown to consist of Archean SCLM, overprinted during Proterozoic to Paleozoic events (Bonadiman et al., 2006; Coltorti et al., 2008). The presence of such SCLM remnants also can help to explain both ancient Re-Os model ages from abyssal peridotites (e.g., Alard et al., 2005) and the isotopic systematics of ocean-island volcanic rocks (O'Reilly et al., 2008). Several of the "deep reservoirs" discussed by isotopic geochemists may in fact reside in relatively shallow remnants of ancient SCLM that can contaminate rising magmas (O'Reilly and Griffin, 2004). The implications of this situation will be explored elsewhere.

Crust–SCLM detachment during rifting has profound ramifications for continental terrane analysis. During the multiple phases of rifting, accretion, and collision involved in supercontinent cycles, younger crust may be deposited on, or thrust over, the buoyant SCLM of small archons and the flanks of larger cratons; several examples are illustrated by a comparison of Figures 1, 2, and 17, as discussed above.

(7) Implications for Earth Dynamics and Continental Evolution

Integration of our knowledge of crustal history with an understanding of the underlying SCLM (composition, age, and velocity characteristics) makes it possible to relate geological events such as subduction-related magmatism, rift magmatism (e.g., the East Africa Rift), and possibly plume magmatism (e.g., the Bushveld Complex), to the processes affecting the SCLM and its modification over time. The integration of continental-scale data sets (e.g., gravity, magnetics, seismic velocity, topography/bathymetry, and geology) in a geographic information system (GIS) environment enables spatial definition of the individual lithospheric domains (summarized in Fig. 2). If our interpretations of Figures 2 and 16 are correct, then the bulk (at least 65%) of the African SCLM is probably of Archean origin but variably metasomatized by subsequent geological events.

This finding is consistent with a dynamic Earth dominated by recycling of juvenile fertile mantle lithosphere (e.g., Armstrong, 1981, 1991). The higher density of such material (Poudjom Djomani et al., 2001) and its relatively hydrous nature (at least in arc settings) are likely to favor its recycling via delamination (e.g., Sobolev et al., 2005). Recycling of fertile mantle lithosphere and preservation of more depleted (buoyant and resistant) Archean SCLM have major implications for models of crustal growth (e.g., Armstrong, 1981; Taylor and McLennan, 1985; Stein and Hoffmann, 1994; Condie, 1998, 2000); we suggest that the surface area of continental SCLM has been relatively constant at least since the end of the Archean.

Combining the interpretation of SCLM domains with our understanding of geological history also enables us to reconstruct the growth history of the African cratons and continent, and to recognize the geodynamic processes implicit in this history (Fig. 14). The rigidity and durability of the depleted Archean SCLM exert a fundamental control on the history of convergent margins and thus on the behavior of plate tectonics. Collisions of cratons, or accretion of microcontinents to cratons, result in transfer of stress and plate rearrangement, and generally initiate consumption of a different oceanic plate (e.g., Cawood and Buchan, 2007). In extreme cases such behavior can cause multiple, sequential switching of convergent margin activity to different sides of a single growing craton, as described above for the Kalahari Craton.

CONCLUSIONS

The lithospheric architecture of Africa provides many insights into the processes of continental assembly and breakup, and the importance of Archean SCLM for continental dynamics. Africa today consists of several Archean cratons and smaller cratonic fragments, stitched together and flanked by younger fold belts. The cratons themselves are aggregates of continental fragments 3.6–2.5 Ga in age, and differ markedly from one another in their structure and evolution. The larger cratons are underlain by geochemically depleted, rigid and mechanically robust SCLM. These cratonic roots have steep sides and locally extend to depths of >300 km and have played a major role in the development of the continental framework. The cratonic margins, and some intracratonic domain boundaries, have repeatedly focused ascending magmas, leading to refertilization of the SCLM. These weakened boundaries have localized repeated cycles of extension, rifting, subduction, and renewed accretion; the ongoing development of the East Africa Rift is only the latest stage in this process. The extension of cratonic roots well into the ocean basins suggests the listric detachment of the upper lithosphere during continental breakup, leading to a scatter of lithospheric fragments in the ocean basins. During the closure of oceans, younger crust may be emplaced on older SCLM, either on these microcontinents or the flanks of larger cratons. The more fertile SCLM that underlies some accretionary belts probably was generated in Archean time, and has been gradually refertilized by the passage of magmas during younger tectonic events. Modified Archean SCLM may thus be far more extensive in Africa than previously estimated. This analysis implies that crustal and lithospheric recycling of post-Archean material during the collision and accretionary process is more important than generally recognized.

ACKNOWLEDGMENTS

We thank Tim Craske for his early contributions in the area of lithospheric mapping and the Senior Management of the former WMC Resources, Ltd, without whose support this work would not have been possible. We also thank BHP Billiton Ltd for their continued support of the project. We are grateful to Norman Pearson for extensive discussions over many years, and to the staff of the GEMOC Geochemical Analysis Unit for helping to generate the large volumes of geochemical data that underlie this work. We thank Albidon Limited for use of their geochronology data from southeast Tanzania. This work has been supported by Discovery, SPIRT, and Linkage grants from the Australian Research Council (S.Y. O'Reilly and W.L. Griffin) and Macquarie University Collaborative Research Grants. Jean-Yves Cottin organized a seminal workshop at Université Jean Monnet (Saint-Étienne), and M. Abdelsalam provided many useful contributions. We thank Mark Schmitz and an anonymous referee for thoughtful reviews that helped us to improve the presentation. This is contribution 547 from the ARC National Key Centre for Geochemical Evolution and Metallogeny of Continents (www.es.mq.edu.au/GEMOC).

REFERENCES CITED

Abdelsalam, M.G., Liègeois, J.-P., and Stern, R.J., 2002, The Saharan Metacraton: Journal of African Earth Sciences, v. 34, p. 119–136, doi: 10.1016/S0899-5362(02)00013-1.

Afonso, J.C., Fernandez, M., Ranalli, G., Griffin, W.L., and Connolly, J.A.D., 2008, Integrated geophysical-petrological modeling of the lithosphere and sublithospheric upper mantle: Methodology and applications: Geochemistry Geophysics Geosystems, v. 9, doi: 10.1029/2007GC001834.

Alard, O., Luguet, A., Pearson, N.J., Griffin, W.L., Lorand, J.-P., Gannoun, A., Burton, K.W., and O'Reilly, S.Y., 2005, In-situ Os isotopes in abyssal peridotites: Bridging the "isotopic gap" between MORB and their source mantle: Nature, v. 436, p. 1005–1008, doi: 10.1038/nature03902.

Anhaeusser, C.R., 1990, Precambrian crust evolution and metallogeny of Southern Africa, *in* Naqvi, S.M., ed., Precambrian continental crust and its economic resources: Amsterdam, Elsevier, p. 123–156.

Appel, P., Schenk, V., and Schumann, A., 2005, P-T path and metamorphic ages of pelitic schists at Murchison Falls, NW Uganda: Evidence for a Pan-African tectonometamorphic event in the Congo Craton: European Journal of Mineralogy, v. 17, p. 655–664, doi: 10.1127/0935-1221/2005/0017-0655.

Armstrong, R.L., 1981, Radiogenic isotopes: The case for crustal recycling on a near steady-state no continental growth Earth: Philosophical Transactions of the

Royal Society, v. A301, p. 443–472, doi: 10.1098/rsta.1981.0122.
Armstrong, R.L., 1991, The persistent myth of crustal growth: Australian Journal of Earth Sciences, v. 38, p. 613–630, doi: 10.1080/08120099108727995.
Armstrong, R.A., Robb, L.J., Master, S., Kruger, F.J., and Mumba, P.A.C.C., 1999, New U-Pb age constraints on the Katangan Sequence, Central African Copperbelt, J. Afr. Earth Sci. Special Abstracts Issue, GSA 11: Earth Resources for Africa, v. 28, p. 6–7.
Attoh, K., and Ekwueme, B.N., 1997, The West African shields, *in* de Wit, M., and Ashwal, L.D., eds., Greenstone belts: Oxford, Clarendon Press, p. 515–527.
Ballentine, C.J., Lee, D-Ch., and Halliday, A.N., 1997, Hafnium isotopic studies of the Cameroon line and new HIMU paradoxes: Chemical Geology, v. 139, p. 111–124.
Barr, M.W.C., Downing, K.N., Harding, A.E., and Loughlin, W.P., 1984, Regional correlation near the junction of the Zambezi and Mozambique belts, east-central Africa: Maputo, Mozambique, Open-File Report, Hunting Geology and Geophysics, Instituto Nacional de Geologia.
Becker, T., and Brandenburg, A., 2002, The petrogenesis of the Alberta Complex within the Rehoboth basement inlier of Namibia: South African Journal of Geology, v. 105, p. 147–162, doi: 10.2113/105.2.147.
Becker, T., and Ledru, P., Garoeb, H., and Milesi, J.P., 2004, The Mesoproterozoic event within the Rehoboth Basement Inlier of Namibia: Review and new aspects of metamorphism, structure, and stratigraphy: Orleans, Abstracts 20th Colloquium of African Geology, p. 70.
Bell, D.R., Schmitz, M.D., and Janney, P.E., 2004, Mesozoic thermal evolution of the southern African lithosphere: Lithos, v. 71, p. 273–287, doi: 10.1016/S0024-4937(03)00117-8.
Bell, D.R., Gregoire, M., Grove, T.L., Chatterjee, N., Carlson, R.W., and Buseck, P.R., 2005, Silica and volatile-element metasomatism of Archean mantle: A xenolith-scale example from the Kaapvaal Craton: Contributions to Mineralogy and Petrology, v. 150, p. 251–267, doi: 10.1007/s00410-005-0673-8.
Beyer, E.E., Griffin, W.L., and O'Reilly, S.Y., 2006, Transformation of Archean lithospheric mantle by refertilization: Evidence from exposed peridotites in the Western Gneiss Region, Norway: Journal of Petrology, v. 47, p. 1611–1636, doi: 10.1093/petrology/egl022.
Black, R., Latouche, L., Liègeois, J.P., Caby, R., and Bertrand, J.M., 1994, Pan-African displaced terranes in the Tuareg shield (Central Sahara): Geology, v. 22, p. 641–644, doi: 10.1130/0091-7613(1994)022<0641:PADTIT>2.3.CO;2.
Blenkinsop, T., Martin, A., Jelsma, H.A., and Vinyu, M.L., 1997, Zimbabwe Craton, *in* de Wit, M., and Ashwal, L.D., eds., Greenstone belts: London, Clarendon Press, p. 567–580.
Boher, M., Abouchami, C.J., Michard, A., Albarede, F., and Arndt, N.T., 1992, Crustal growth in West Africa at 2.1 Ga: Journal of Geophysical Research, v. 97, p. 345–369, doi: 10.1029/91JB01640.
Bonadiman, C., Coltorti, M., Siena, F., O'Reilly, S.Y., Griffin, W.L., and Pearson, N.J., 2006, Archean to Proterozoic depletion in Cape Verde lithospheric mantle: Geochimica et Cosmochimica Acta, v. 70, supplement 1, p. A58, doi: 10.1016/j.gca.2006.06.221.
Borg, G., and Shackelton, R.M., 1997, The Tanzania and NE-Zaire cratons, *in* de Wit, M., and Ashwal, L.D., eds., Greenstone belts: London, Clarendon Press, p. 608–619.
Boven, A., Theunissen, K., Sklyariv, E., Klerkx, J., Melnikov, A., Mruma, A., and Punzalan, L., 1999, Timing of exhumation of a high-pressure mafic granulite terrane of the Paleoproterozoic Ubende belt (West Tanzania): Precambrian Research, v. 93, p. 119–137, doi: 10.1016/S0301-9268(98)00101-6.
Brandl, G., and de Wit, M.J., 1997, The Kaapvaal Craton, *in* de Wit, M., and Ashwal, L.D., eds., Greenstone belts: London, Clarendon Press, p. 581–607.
Bruguier, O., Dada, S., and Lancelot, J.R., 1994, Early Archean component (>3.5 Ga) within 3.05 Ga orthogneiss from northern Nigeria: U-Pb zircon evidence: Earth and Planetary Science Letters, v. 125, p. 89–103, doi: 10.1016/0012-821X(94)90208-9.
Bulambo, M., De Waele, B., Kampunzu, A.B., and Tembo, F., 2004, SHRIMP U-Pb geochronology of the Choma-Kalomo block (Zambia) and geological implications: Orleans, Abstracts 20th Colloquium of African Geology, p. 96.
Burke, K., Ashwal, L.D., and Webb, S.J., 2003, A new way to map old sutures using deformed alkaline rocks and carbonatites: Geology, v. 31, p. 391–394, doi: 10.1130/0091-7613(2003)031<0391:NWTMOS>2.0.CO;2.
Caby, R., 2003, Terrane assembly and geodynamic evolution of central-western Hoggar: A synthesis: Journal of African Earth Sciences, v. 37, p. 133–159, doi: 10.1016/j.jafrearsci.2003.05.003.
Cahen, L., Snelling, N.J., Delhail, J., and Vail, J.R., 1984, The geochronology and evolution of Africa: London, Clarendon Press, 512 p.
Carlson, R.W., Pearson, D.G., Boyd, F.R., Shirey, S.B., Irvine, G., Menzies, A.H., and Gurney, J.J., 1999, Re-Os systematics of lithospheric peridotites: Implications for lithosphere formation and preservation: Cape Town, Proceedings 7th International Kimberlite Conference, Red Roof Design, p. 99–108.
Carvalho, H. De., Tassinari, C., Alves, P.H., Guimaraes, F., and Simöes, M.C., 2000, Geochronological review of the Precambrian in western Angola: Links with Brazil: J. African Earth Sci., v. 31, p. 383 402.
Cawood, P.A., and Buchan, C., 2007, Linking accretionary orogenesis with supercontinent assembly: Earth-Science Reviews, v. 82, p. 217–256, doi: 10.1016/j.earscirev.2007.03.003.
Chesley, J.T., Rudnick, R.L., and Lee, C.T., 1999, Re-Os systematics of mantle xenoliths from the East African Rift: Age, structure, and history of the Tanzanian craton: Geochimica et Cosmochimica Acta, v. 63, p. 1203–1217, doi: 10.1016/S0016-7037(99)00004-6.
Chevrot, S., and Zhao, L., 2007, Multiscale finite-frequency Raleigh wave tomography of the Kaapvaal craton: Geophysical Journal International, v. 169, p. 201–215, doi: 10.1111/j.1365-246X.2006.03289.x.
Coltorti, M., Bonadiman, C., O'Reilly, S.Y., Griffin, W.L., and Pearson, N., 2008, Heterogeneity in the oceanic lithosphere as evidenced by mantle xenoliths from Sal Island (Cape Verde Archipelago): Abstract, 33rd International Geological Congress, session EIL-03.
Condie, K.C., 1998, Episodic continental growth and supercontinents: A mantle avalanche connection?: Earth and Planetary Science Letters, v. 163, p. 97–108.
Condie, K.C., 2000, Episodic continental growth models: Afterthoughts and extensions: Tectonophysics, v. 322, p. 153–162, doi: 10.1016/S0040-1951(00)00061-5.
Cornell, D.H., Armstrong, R.A., and Walraven, F., 1998, Geochronology of the Proterozoic Hartley Basalt Formation, South Africa: Constraints on the Kheis tectogenesis and the Kaapvaal Craton's earliest Wilson cycle: Journal of African Earth Sciences, v. 26, p. 5–27, doi: 10.1016/S0899-5362(97)00133-4.
Cutten, H., Fernandez-Alonso, M., de Waele, B., and Tack, L., 2004, Age constraints for basin evolution and sedimentation in the "Northeastern Kibaran Belt": Orleans, Abstracts, 20th Colloquium of African Geology, p. 123.
Dallmeyer, R.D., 1989, Contrasting accreted terranes in the southern Appalachian Orogen, basement beneath the Atlantic and Gulf Coastal Plains and West African Orogens: Precambrian Research, v. 42, p. 387–409, doi: 10.1016/0301-9268(89)90021-1.
Dalziel, I.W., Mosher, S., and Gahagan, L.M., 2000, Laurentia-Kalahari collision and the assembly of Rodinia: The Journal of Geology, v. 108, p. 499–513, doi: 10.1086/314418.
Danchin, R.V., 1979, Mineral and bulk chemistry of garnet lherzolite and garnet harzburgite xenoliths from the Premier mine, South Africa, *in* Boyd, F.R., and Meyer, H.O.A., eds., The mantle sample: Inclusions in kimberlites and other volcanics: Washington, D.C, American Geophysical Union, p. 104–126.
Dean, S.M., Minshull, T.A., Whitmarsh, R.B., and Louden, K.E., 2000, Deep structure of the ocean-continent transition in the southern Iberia Abyssal Plain from seismic refraction profiles: The IAM-9 transect at 40°20′N: Journal of Geophysical Research, v. 105, B3, p. 5859–5885, doi: 10.1029/1999JB900301.
Debayle, E., and Kennett, B., 2000, Anisotropy in the Australasian upper mantle from Love and Rayleigh waveform inversion: Earth and Planetary Science Letters, v. 184, p. 339–351, doi: 10.1016/S0012-821X(00)00314-9.
De Carvalho, H., Tassinari, C., Alves, P.H., Guimaraes, F., and Simöes, M.C., 2000, Geochronological review of the Precambrian in western Angola: Links with Brazil: Journal of African Earth Sciences, v. 31, p. 383–402, doi: 10.1016/S0899-5362(00)00095-6.
Deen, T., Griffin, W.L., Begg, G., O'Reilly, S.Y., and Natapov, L.M., 2006, Thermal and compositional structure of the subcontinental lithospheric mantle: Derivation from shear-wave seismic tomography: Geochemistry Geophysics Geosystems, doi: 10.1029/2005GC001164.
De Waele, B., 2005, The Proterozoic geological history of Irumide belt, Zambia [Ph.D. thesis]: Perth, Australia, Curtin University of Technology, 358 p.
De Waele, B., and Fitzsimons, I.C.W., 2004, The age and detrital fingerprint of the Muva Supergroup of Zambia: Molassic deposition to the southwest of the Ubendian Belt: Geoscience Africa, Abstracts, p. 162–163.
De Waele, B., and Mapani, B., 2002, Geology and correlation of the central Irumide belt: Journal of African Earth Sciences, v. 35, p. 385–397, doi: 10.1016/S0899-5362(02)00149-5.
De Waele, B., Wingate, M.T.D., Mapani, B.S.E., and Fitzsimons, I.C.W., 2003, Untying the Kibaran knot: A reassessment of Mesoproterozoic correlations in southern Africa based on SHRIMP U-Pb data from the Irumide belt: Geology, v. 31, p. 509–512, doi: 10.1130/0091-7613(2003)031<0509:UTKKAR>2.0.CO;2.
De Wit, M.J., 1998, On Archean granites, greenstones, cratons and tectonics: Does the evidence demand a verdict?: Precambrian Research, v. 91, p. 181–224, doi: 10.1016/S0301-9268(98)00043-6.
Dirks, P.H.G.M., and Jelsma, H.A., 2002, Crust-mantle decoupling and the growth of the Archaean Zimbabwe craton: Journal of African Earth Sciences, v. 34, p. 157–166, doi: 10.1016/S0899-5362(02)00015-5.
Duchesne, J.-C., Liègeois, J.-P., Deblond, A., and Tack, L., 2004, Petrogenesis of the Kabanda-Musongati layered mafic-ultramafic intrusions in Burundi (Kibaran Belt): Geochemical Sr-Nd isotopic constraints and Cr-Ni behavior: Journal of African Earth Sciences, v. 39, p. 133–145, doi: 10.1016/j.jafrearsci.2004.07.055.
Ebinger, C.J., and Sleep, N.H., 1998, Cenozoic magmatism throughout east Africa resulting from impact of a single plume: Nature, v. 395, p. 788–791, doi: 10.1038/27417.
Eglington, B.M., 2006, Evolution of the Namaqua-Natal Belt, southern Africa—A geochronological and isotope geochemical review: Journal of African Earth Sciences, v. 46, p. 93–111, doi: 10.1016/j.jafrearsci.2006.01.014.
Faure, S., 2006, World kimberlites database, Version 2006-2: Consortium de Recherche en Exploration Minérale CONSOREM, (www.consorem.ca), Université du Québec à Montréal.
Ferré, E., Déléri, J., Bouchez, J.-L., Lar, A.U., and Peucat, J.-J., 1996, The Pan-African reactivation of Eburnean and Archean provinces in Nigeria: Structural and isotopic data: Journal of the Geological Society, v. 153, p. 719–728, doi: 10.1144/gsjgs.153.5.0719.
Ferré, E., Gleizes, G., and Caby, R., 2002, Obliquely convergent tectonics and granite emplacement in the Trans-Saharan belt in Eastern Nigeria: A synthesis: Precambrian Research, v. 114, p. 199–219, doi: 10.1016/S0301-9268(01)00226-1.
Feybesse, J.L., Johan, V., Triboulet, C., Guerrot, C., Mayaga-Mikolo, F., Bouchot, V., and N'Dong, J., 1998, The West Central African belt: A model of 2.5–2.0 Ga accretion and two-phase orogenic evolution: Precambrian Research, v. 87, p. 161–216, doi: 10.1016/S0301-9268(97)00053-3.
Fitton, J.G., and Dunlop, H.M., 1985, The Cameroon line, West Africa, and its bearing on the origin of oceanic and continental alkali basalt: Earth and Planetary Science Letters, v. 72, p. 23–38, doi: 10.1016/0012-821X(85)90114-1.
Fouch, M.J., James, D.E., VanDecar, J.C., van der Lee, S., and The Kaapvaal Seismic Group, 2004, Mantle seismic structure beneath the Kaapvaal and Zimbabwe Cratons: South African Journal of Geology, v. 107, p. 33–44, doi: 10.2113/107.1-2.33.
Frei, R., Blenkinsop, T.G., and Shönberg, R., 1999, Geochronology of the late Archean Razi and Chilimanzi suites of granites in Zimbabwe: Implications for the late Archean

tectonics of the Limpopo belt and Zimbabwe craton: South African Journal of Geology, v. 102, p. 55–63.
Frimmel, H.E., Zartman, R.E., and Späth, A., 2001, The Richtersveld igneous complex, South Africa: U-Pb zircon and geochemical evidence for beginning of Neoproterozoic continental break-up: The Journal of Geology, v. 109, p. 493–522, doi: 10.1086/320795.
Gaul, O.F., Griffin, W.L., O'Reilly, S.Y., and Pearson, N.J., 2000, Mapping olivine composition in the lithospheric mantle: Earth and Planetary Science Letters, v. 182, p. 223–235, doi: 10.1016/S0012-821X(00)00243-0.
Goes, S., and van der Lee, S., 2002, Thermal structure of the North American uppermost mantle interred from seismic topography: Journal of Geophysical Research, v. 107, doi: 10.1029/2000JB000049.
Goodwin, A.M., 1996: Principles of Precambrian geology: London, Academic Press, 327 p.
Goscombe, B., Armstrong, R.A., and Barton, J.M., 2000, Geology of the Chewore Inliers, Zimbabwe: Constraining the Mesoproterozoic to Paleozoic evolution of the Zambezi belt: Journal of African Earth Sciences, v. 30, p. 589–627, doi: 10.1016/S0899-5362(00)00041-5.
Grand, S., 2002, Mantle shear-wave tomography and the fate of subducted slabs: Philosophical Transactions of the Royal Society of London, v. A360, p. 2475–2491.
Grand, S.P., 1994, Mantle shear structure beneath the Americas and surrounding oceans: Journal of Geophysical Research, v. 99, p. 11,591–11,621.
Grand, S.P., van der Hilst, R.D., and Widiyantoro, S., 1997, Global seismic tomography: A snapshot of convection in the Earth: GSA Today, v. 7, p. 1–7.
Griffin, W.L., and O'Reilly, S.Y., 2007, The earliest subcontinental mantle, *in* Van Kranendonk, M., Smithies, H., and Bennett, V., eds., Earth's oldest rocks: Amsterdam, Elsevier, p. 1013–1035.
Griffin, W.L., Ryan, C.G., O'Reilly, S.Y., Nixon, P.H., and Win, T.T., 1994, Trace elements in garnets from Tanzanian kimberlites: Relation to diamond content and tectonic setting, *in* Meyer, H.O.A., and Leonardos, O.H., eds., Diamonds: Characterization, genesis and exploration: Companhia de Pesquisa de Recursos Minerais (CPRM) Special Publication 1B/93, p. 346–358.
Griffin, W.L., O'Reilly, S.Y., Ryan, C.G., Gaul, O., and Ionov, D., 1998, Secular variation in the composition of subcontinental lithospheric mantle, *in* Braun, J., Dooley, J.C., Goleby, B.R., van der Hilst, R.D., and Klootwijk, C.T., eds., Structure and evolution of the Australian continent: Washington D.C., American Geophysical Union, Geodynamics, v. 26, p. 1–26.
Griffin, W.L., O'Reilly, S.Y., and Ryan, C.G., 1999, The composition and origin of subcontinental lithospheric mantle, *in* Fei, Y., Bertka, C.M., and Mysen, B.O., eds., Mantle petrology: Field observations and high-pressure experimentation: A tribute to Francis R. (Joe) Boyd: Houston, Geochemical Society Special Publication No. 6, p. 13–45.
Griffin, W.L., Spetsius, Z.V., Pearson, N.J., and O'Reilly, S.Y., 2002, In-situ Re-Os analysis of sulfide inclusions in kimberlitic olivine: New constraints on depletion events in the Siberian lithospheric mantle: Geochemistry Geophysics Geosystems, v. 3, no. 1069.
Griffin, W.L., O'Reilly, S.Y., Natapov, L.M., and Ryan, C.G., 2003a, The evolution of lithospheric mantle beneath the Kalahari Craton and its margins: Lithos, v. 71, p. 215–241, doi: 10.1016/j.lithos.2003.07.006.
Griffin, W.L., O'Reilly, S.Y., Abe, N., Aulbach, S., Davies, R.M., Pearson, N.J., Doyle, B.J., and Kivi, K., 2003b, The origin and evolution of Archean lithospheric mantle: Precambrian Research, v. 127, p. 19–41, doi: 10.1016/S0301-9268(03)00180-3.
Griffin, W.L., Graham, S., O'Reilly, S.Y., and Pearson, N.J., 2004, Lithosphere evolution beneath the Kaapvaal Craton Re-Os systematics of sulfides in mantle-derived peridotites: Chemical Geology, v. 208, p. 89–118, doi: 10.1016/j.chemgeo.2004.04.007.
Griffin, W.L., Belousova, E., Ketchum, J., Beyer, E., and Saeed, A., 2005, TerraneChron®: Analysis of six samples from Botswana: GEMOC Report for WMC Resources WMS/05–02, 10 p.
Griffin, W.L., O'Reilly, S.Y., Afonso, J.C., and Begg, G.C., 2008, The composition and evolution of lithospheric mantle: A re-evaluation and its tectonic implications: Journal of Petrology, doi: 10.1093/petrology/egn033.
Gung, Y., Panning, M., and Romanowicz, B., 2003, Global anisotropy and the thickness of continents: Nature, v. 422, p. 707–711, doi: 10.1038/nature01559.
Gurnis, M., Mitrovica, J.X., Ritsema, J., and van Heijst, H.J., 2000, Constraining mantle density structure using geological evidence of surface uplift rates: The case of the African Superplume: Geochemistry Geophysics Geosystems, v. 1, p. 127–142, doi: 10.1029/1999GC000035.
Hacker, B.R., and Abers, G.A., 2004, Subduction Factory 3: An Excel worksheet and macro for calculating the densities, seismic wave speeds, and H_2O contents of minerals and rocks at pressure and temperature: Geochemistry Geophysics Geosystems, v. 5, doi: 10.1029/2003GC000614.
Haddoum, H., Choukroune, P., and Peucat, J.J., 1994, Evolution of the Precambrian In-Ouzzal block (Central Sahara, Algeria): Precambrian Research, v. 65, p. 155–166, doi: 10.1016/0301-9268(94)90103-1.
Hanson, R.E., 2003, Proterozoic geochronology and tectonic evolution of southern Africa, *in* Yoshida, M., Windley, B.F., and Dasgupta, S., eds., Proterozoic east Gondwana: Supercontinent assembly and breakup: The Geological Society of London, Special Publication, v. 206, p. 427–463.
Hanson, R.E., Wilson, T.J., and Wardlaw, M.S., 1988, Deformed batholiths in the Pan-African Zambezi Belt, Zambia: Age and implications for regional Proterozoic tectonics: Geology, v. 16, p. 1134–1137, doi: 10.1130/0091-7613(1988)016<1134:DBITPA>2.3.CO;2.
Hanson, R.E., Hargrove, U.S., Martin, M.W., Bowring, S.A., Krol, M.A., Hodges, K.V., Munyanyiwa, H., and Blenkinsop, T.G., 1998, New geochronological constraints on the tectonic evolution of the Pan-African Zambezi belt, south-central Africa: Journal of African Earth Sciences, v. 27, p. 104–105.
Hargrove, S.U., Hanson, R.E., Martin, M.E., Blenkinsop, K.G., Bowring, S.A., Walker, N., and Munyanyiwa, H., 2003, Tectonic evolution of the Zambezi orogenic belt: Geochronological, structural, and petrological constraints from northern Zimbabwe: Precambrian Research, v. 123, p. 159–186, doi: 10.1016/S0301-9268(03)00066-4.
Hartnady, C., Joubert, P., and Stowe, C., 1985, Proterozoic crustal evolution in southwestern Africa: Episodes, v. 8, p. 236–243.
Hoal, B.G., and Heaman, L.M., 1995, The Sinclair Sequence: U-Pb age constraints from the Awasib Mountains area: Communications Geological Survey of Namibia, v. 10, p. 83–91.
Hoal, K.O., 2004, Samples of Proterozoic iron-enriched mantle from the Premier kimberlite: Lithos, v. 71, p. 259–272, doi: 10.1016/S0024-4937(03)00116-6.
Hofmann, A., Kröner, A., and Brandl, G., 1998, Field relationships of mid- to late-Archean high-grade gneisses of igneous and sedimentary parentage in the Sand River, Central Zone of the Limpopo Belt, South Africa: South African Journal of Geology, v. 101, p. 185–200.
Holzer, L., Frei, R., Barton, J.M., Jr., and Kramers, J.R., 1998, Unraveling the record of successive high grade events in the Central zone of the Limpopo belt using Pb single phase dating of metamorphic minerals: Precambrian Research, v. 87, p. 87–115, doi: 10.1016/S0301-9268(97)00058-2.
Huismans, R.S., and Beaumont, C., 2008, Complex rifted continental margins explained by dynamical models of depth-dependent lithospheric extension: Geology, v. 36, p. 163–166, doi: 10.1130/G24231A.1.
Jacobs, J., and Thomas, R.J., 1994, Oblique collision at about 1.1 Ga along the southern margin of the Kaapvaal continent, southeast Africa: Geologische Rundschau, v. 83, p. 322–333.
Jacobs, J., Falter, M., Thomas, R.J., Kunz, J., and Jeberger, E.K., 1997, $^{40}Ar/^{39}Ar$ thermochronological constraints on the structural evolution of the Mesoproterozoic Natal Metamorphic Province, SE Africa: Precambrian Research, v. 86, p. 71–92, doi: 10.1016/S0301-9268(97)00042-9.
James, D.E., Fouch, M.J., VanDecar, J.C., van der Lee, S., and Kaapvaal Seismic Group, 2001, Tectospheric structure beneath southern Africa: Geophysical Research Letters, v. 28, p. 485–488, doi: 10.1029/2000GL012578.
James, D.E., Boyd, F.R., Schutt, D., Bell, D.R., and Carlson, R.W., 2004, Xenolith constraints on seismic velocities in the upper mantle beneath southern Africa: Geochemistry Geophysics Geosystems, v. 5, doi: 10.1029/2003GC000551.
Janse, A.J.A., 1994, Is Clifford's Rule still valid? Affirmative examples from around the world, *in* Meyer, H.O.A., and Leonardos, O.H., eds., Diamonds: Characterization, genesis and exploration: Brazilia, Departement Nacional da Production Mineralia, p. 215–235.
Jaques, A.L., and Milligan, P.R., 2004, Patterns and controls on the distribution of diamondiferous intrusions in Australia: Lithos, v. 77, p. 783–802, doi: 10.1016/j.lithos.2004.03.042.
John, T., Schenk, V., Hause, K., Scherer, E.E., and Tembo, F., 2003, Evidence for a Neoproterozoic ocean in central-south Africa from mid-oceanic-ridge-type geochemical signatures and pressure-temperature estimates of Zambian eclogites: Geology, v. 31, p. 243–246, doi: 10.1130/0091-7613(2003)031<0243:EFANOI>2.0.CO;2.
Johnson, S.P., and Rivers, T., 2004, Review of the Mesoproterozoic to early Paleozoic magmatic and tectonothermal history of central southern Africa: Implications for Rodinia and Gondwana: Geoscience Africa, v. 2004, p. 309–310.
Johnson, S.P., Rivers, T., and De Waele, B., 2005, A review of the Mesoproterozoic to Early Paleozoic magmatic and tectonothermal history of Central Southern Africa: Implications for Rodinia and Gondwana: Journal of the Geological Society, v. 162, p. 433–450, doi: 10.1144/0016-764904-028.
Kampunzu, A.B., Tembo, F., Matheis, G., Kapenda, D., and Huntsman-Mapila, P., 2000, Geochemistry and tectonic setting of mafic igneous units in the Neoproterozoic Katangan basin, Central Africa: Implications for Rodinia break-up: Gondwana Research, v. 3, p. 125–153, doi: 10.1016/S1342-937X(05)70093-9.
Katongo, C., Koller, F., Kloetzli, U., Koeberl, C., Tembo, F., and De Waele, B., 2004, Petrography, geochemistry, and geochronology of granitoid rocks in the Neoproterozoic-Paleozoic Lufilian-Zambezi belt, Zambia: Implications for tectonic setting and regional correlation: Journal of African Earth Sciences, v. 40, p. 219–244, doi: 10.1016/j.jafrearsci.2004.12.007.
Kazmin, V.G., 2002, Precambrian tectonics and geodynamics of Namibia, *in* Mezhelovsy, L., ed., Prospective fields of geological, geodynamic and metallogenic investigations in Namibia: Scientific and applied aspects: Moscow, Inter-regional Centre for Geological Cartography Russia, p. 57–77.
Key, R.M., Liyungu, A.K., Njamu, F.M., Somwe, V., Banda, J., Mosley, P.N., and Armstrong, R.A., 2001, The western arm of the Lufilian Arc in NW Zambia and its potential for copper mineralization: Journal of African Earth Sciences, v. 33, p. 503–528, doi: 10.1016/S0899-5362(01)00098-7.
Kieffer, B., Arndt, N., Lapierre, H., Bastieni, F., Bosh, D., Pecher, A., Yirgu, G., Ayalew, D., Weis, D., Jerram, D.A., Keller, F., and Meugnot, C., 2004, Flood and shield basalts from Ethiopia: Magmas from the African Superswell: Journal of Petrology, v. 45, p. 793–834, doi: 10.1093/petrology/egg112.
Klerkx, J., Liegeois, J.P., Lavreau, J., and Classens, W., 1987, Crustal evolution of the northern Kibaran belt, eastern and central Africa, *in* Kröher, A., ed., Proterozoic lithospheric evolution: Washington, D.C., American Geophysical Union, Geodynamics Series, v. 17, p. 217–233.
Kokonyangi, J., Armstrong, R., Kampunzu, A.B., Yoshida, M., and Okudaira, T.R., 2004, U-Pb zircon geochronology and petrology of granitoids from Mitwaba (Katanga, Congo): Implications for the evolution of the Mesoproterozoic Kibaran belt: Precambrian Research, v. 132, p. 79–106, doi: 10.1016/j.precamres.2004.02.007.
Kokonyangi, J., Kampunzu, A.B., Poujol, M., Okudaira, T., Yoshida, M., and Shabeer, K.P., 2005, Petrology and geochronology of Mesoproterozoic mafic-intermediate plutonic rocks from Mitwaba (D.R. Congo): Implications for the evolution of the Kibaran belt in central Africa: Geological Magazine, v. 142, p. 109–130, doi: 10.1017/S0016756804009951.
Korhonen, J.V., Farihead, J.D., Hamoudi, M., Hemant, K., Lesur, V., Mandea, M., Maus, S., Purucker, M., Ravat, D., Sazonova, T., and Thébault, E., 2007, Magnetic anomaly map of the world: Commission for the Geological Map of the World.

Kouamelan, A.N., Peucat, J.J., and Delor, C., 1997, Archean (3.15 Ga) relics at the heart of Birrimian (2.1 Ga) magmatism in the Ivory Coast, West African Craton: Comptes Rendus de l'Academie des Sciences, Series II, Sciences de la Terre et des Planets, v. 324, p. 719–727.

Kreissig, K.L., Holzer, L.R., Frei, R., Villa, I.M., Kramersa, J.D., Kröner, A., Smith, C.A., and van Reenen, V.V., 2001, Geochronology of the Hout River shear zone and the metamorphism in the Southern Marginal Zone of the Limpopo Belt, Southern Africa: Precambrian Research, v. 109, p. 145–173, doi: 10.1016/S0301-9268(01)00147-4.

Kröner, A., and Tegtmeyer, A., 1994, Gneiss-greenstone relationships in the Archean Gneiss Complex of south-western Swaziland, southern Africa and implications for early crustal evolution: Precambrian Research, v. 67, p. 109–139, doi: 10.1016/0301-9268(94)90007-8.

Kröner, A., Sacchi, R., Jaeckel, P., and Costa, M., 1997, Kibaran magmatism and Pan-African granulite metamorphism in northern Mozambique: Single zircon ages and regional implications: Journal of African Earth Sciences, v. 25, p. 467–484, doi: 10.1016/S0899-5362(97)00117-6.

Kröner, A., Willner, A.P., Hegner, E., Jaeckel, P., and Nemchin, A., 2001, Single zircon ages, PT evolution and Nd isotopic systematics of high-grade gneisses in southern Malawi and their bearing on the evolution of the Mozambique belt in southeastern Africa: Precambrian Research, v. 109, p. 257–291, doi: 10.1016/S0301-9268(01)00150-4.

Lawrence, S.R., Munday, S., and Bray, R., 2002, Regional geology and geophysics of the eastern Gulf of Guinea (Niger delta to Rio Muni): Tulsa, Oklahoma, Leading Edge, v. 21, p. 1112–1117, doi: 10.1190/1.1523752.

Lee, C.T., and Rudnick, R.L., 1999, Compositionally stratified cratonic lithosphere: Petrology and geochemistry of peridotite xenoliths from the Labait volcano, Tanzania, *in* Gurney, J.J., et al., eds., Proceedings of VIIth International Kimberlite Conference: Cape Town, Red Roof Design, p. 503– 521.

Lee, D.-Ch., Halliday, A.N., Fitton, J.G., and Poli, G., 1994, Isotopic variations with distance and time in volcanic islands of the Cameroon Line: Evidence of a mantle plume: Earth and Planetary Science Letters, v. 123, p. 119–138, doi: 10.1016/0012-821X(94)90262-3.

Lenardic, A., Moresi, L., and Muehlhaus, H., 2000, The role of mobile belts for the longevity of deep cratonic lithosphere: The crumple zone model: Geophysical Research Letters, v. 27, p. 1235–1238, doi: 10.1029/1999GL008410.

Lenoir, J.L., Liegeois, J.-P., Theunissen, K., and Klerkx, J., 1994, The Paleoproterozoic Ubendian shear belt in Tanzania: Geochronology and structure: Journal of African Earth Sciences, v. 19, p. 169–184, doi: 10.1016/0899-5362(94)90059-0.

Li, A., and Burke, K., 2006, Upper mantle structure of southern Africa from Rayleigh wave tomography: Journal of Geophysical Research, v. 111, doi: 10.1029/2006JB004321.

Lièggeois, J.P., Latouche, L., Boughrara, M., Navez, J., and Guiraud, M., 2003, The LATEA metacraton (Central Hoggar, Tuareg shield): Behaviour of an old passive margin during the pan-African orogeny: Journal of African Earth Sciences, v. 37, p. 161–190, doi: 10.1016/j.jafrearsci.2003.05.004.

Lithgow-Bertelloni, C., and Silver, P.G., 1998, Dynamic topography, plate driving forces and the African Superswell: Nature, v. 395, p. 269–272, doi: 10.1038/26212.

Loose, D., Schenk, V., Schumann, A., and Tiberindwa, J., 2004, Pan-African UHP-metamorphism at the eastern border of the Congo Craton, Labwor Hills, Uganda: Orleans, Abstracts 20th Colloquium of African Geology, p. 268.

Maboko, M.A.H., and Nakamura, E., 1996, Nd and Sm isotopic mapping of the Archean-Proterozoic boundary in southeastern Tanzania using granites as probes for crustal growth: Precambrian Research, v. 77, p. 105–115, doi: 10.1016/0301-9268(95)00048-8.

Manya, S., and Maboko, M.A.H., 2003, Dating basaltic volcanism in the Neoarchaean Sukumaland greenstone belt of the Tanzania Craton using the Sm-Nd method: Implications for the geological evolution of the Tanzania Craton: Precambrian Research, v. 121, p. 35–45, doi: 10.1016/S0301-9268(02)00195-X.

Mapani, B.S.E., Rivers, T., Tembo, F., and Katongo, C., 2001, Terrane mapping in the eastern Irumide and Mozambique belts: Implications for the assembly and dispersal of Rodinia, *in* McCourt, S., ed.: Durban, South Africa, International Geoscience Programme 418, 4th Field Meeting, University of Durban-Westville.

Mapani, B.S.E., Rivers, T., Tembo, F., De Waele, B., and Katongo, S., 2004, Growth of the Irumide terranes and slices of Archean age in Eastern Zambia: Johannesburg, Extended Abstracts, Geoscience Africa, v. 2004, p. 414–415.

Mapeo, R.B.M., Kampunzu, A.B., Armstrong, R.A., and Ramokate, L.V., 2004, SHRIMP U-Pb zircon ages of granitoids from the Kraaipan granite-greenstone terrane of SE Botswana: Implications for the evolutions of the northwestern edge of the Kaapvaal craton: Orleans, Abstracts, 20th Colloquium of African Geology, p. 279.

Meyers, J.B., Rosendahl, B.R., Groshel-Becker, H., Austin, J.A., Jr., and Rona, P.A., 1996, Deep penetrating MCS imaging of the rift-to-drift transition, offshore Daula and North Gabon basins, West Africa: Marine and Petroleum Geology, v. 13, p. 791–835, doi: 10.1016/0264-8172(96)00030-X.

Möller, A., Appel, P., Mezger, K., and Schenk, V., 1995, Evidence for 2 Ga subduction zone: Eclogites in the Usagaran belt in Tanzania: Geology, v. 23, p. 1067–1070, doi: 10.1130/0091-7613(1995)023<1067:EFAGSZ>2.3.CO;2.

Mooney, W.D., Laske, G., and Masters, T.G., 1998, Crust 5.1: A global crustal model at 5° × 5°: Journal of Geophysical Research, v. 103, p. 727–748, doi: 10.1029/97JB02122.

Muhongo, S., Tuisku, P., Mnali, S., Temu, E., Appel, P., and Stendal, H., 2002, High-pressure granulite-facies metagabbros in the Ubendian Belt of SW Tanzania: Preliminary petrography and P-T estimates: Journal of African Earth Sciences, v. 34, p. 279–285, doi: 10.1016/S0899-5362(02)00026-X.

Nyblade, A.A., and Langston, C.A., 1998, Upper mantle P wave velocities beneath southern Africa and the origin of the African superswell: South African Geophysical Review, v. 2, p. 55–61.

Nyblade, A.A., and Robinson, S.W., 1994, The African superswell: Geophysical Research Letters, v. 21, p. 765–768, doi: 10.1029/94GL00631.

Oliver, G.J.H., Johnson, S.P., Williams, I.S., and Herd, D.A., 1998, Relict 1.4 Ga oceanic crust in the Zambezi Valley, northern Zimbabwe: Evidence for the Mid-Proterozoic supercontinental fragmentation: Geology, v. 26, p. 571–573, doi: 10.1130/0091-7613(1998)026<0571:RGOCIT>2.3.CO;2.

O'Neill, C.J., Moresi, L., and Jaques, A.L., 2005, Geodynamic controls on diamond deposits: Implications for Australian occurrences: Tectonophysics, v. 404, p. 217–236, doi: 10.1016/j.tecto.2005.04.010.

O'Reilly, S.Y., and Griffin, W.L., 1985, A xenolith-derived geotherm for southeastern Australia and its geophysical implications: Tectonophysics, v. 111, p. 41–63, doi: 10.1016/0040-1951(85)90065-4.

O'Reilly, S.Y., and Griffin, W.L., 1996, 4-D lithospheric mapping: A review of the methodology with examples: Tectonophysics, v. 262, p. 3–18, doi: 10.1016/0040-1951(96)00010-8.

O'Reilly, S.Y., and Griffin, W.L., 2004, Origin and evolution of continental lithospheric mantle: Buoyant blobs, intracratonic eddies, and fertile upwellings: Florence, Italy, Extended Abstracts, 17th International Geological Congress.

O'Reilly, S.Y., and Griffin, W.L., 2006, Imaging chemical and thermal heterogeneity in the sub-continental lithospheric mantle: Geophysical implications: Tectonophysics, v. 416, p. 289–309, doi: 10.1016/j.tecto.2005.11.014.

O'Reilly, S.Y., Griffin, W.L., Poudjom Djomani, Y.H., and Morgan, P., 2001, Are lithospheres forever?: Tracking changes in subcontinental lithospheric mantle through time: GSA Today, v. 11, p. 4–10, doi: 10.1130/1052-5173(2001)011<0004:ALFTCI>2.0.CO;2.

O'Reilly, S.Y., Griffin, W.L., Zhang, M., and Begg, G., 2008, Archean lithospheric mantle: Its formation, its composition and today's refertilized remains: Frankfurt, Extended Abstract, no. 9IKC-A-00085, 9th International Kimberlite Conference (www.9ikc.com).

Pearson, N.J., Alard, O., Griffin, W.L., Jackson, S.E., and O'Reilly, S.Y., 2002, In situ measurement of Re-Os isotopes in mantle sulfides by laser ablation multi-collector inductively-coupled mass spectrometry: Analytical methods and preliminary results: Geochimica et Cosmochimica Acta, v. 66, p. 1037–1050, doi: 10.1016/S0016-7037(01)00823-7.

Peltonen, P., Manttari, I., Huhma, H., and Kontinen, A., 2003, Archean zircons from the mantle: The Joruma ophiolite revisited: Geology, v. 31, p. 645–648, doi: 10.1130/0091-7613(2003)031<0645:AZFTMT>2.0.CO;2.

Peucat, J.J., Drareni, A., Latouche, L., Deloule, E., and Vidal, P., 2003, U-Pb zircon (TIMS and SIMS) and Sm-Nd whole-rock geochronology of the Gour-Oumelalen granulitic basement, Hoggar massif, Tuareg shield, Algeria: Journal of African Earth Sciences, v. 37, p. 229–239, doi: 10.1016/j.jafrearsci.2003.03.001.

Pickup, S.L.B., Whitmarsh, R.B., Fowler, C.M.R., and Reston, T.J., 1996, Insight into the nature of the ocean-continent transition off West Iberia from a deep multichannel seismic reflection profile: Geology, v. 24, p. 1079–1082, doi: 10.1130/0091-7613(1996)024<1079:IITNOT>2.3.CO;2.

Pin, C., and Poidevin, J.L., 1987, U-Pb zircon evidence for Pan African granulite facies metamorphism in the central African Republic: A new interpretation of the high grade series of the northern border of Congo Craton: Precambrian Research, v. 36, p. 303–331, doi: 10.1016/0301-9268(87)90027-1.

Pinna, P., Journalde, G., Calvez, J.Y., Mroz, J.P., and Marques, J.M., 1993, The Mozambique Belt in northern Mosambique: Neoproterozoic (1100–850 Ma) crustal growth and tectogenesis, and superimposed Pan-African (800–550 Ma) tectonism: Precambrian Research, v. 62, p. 1–59, doi: 10.1016/0301-9268(93)90093-H.

Pinna, P., Cocherie, A., Thiéblemont, D., Jezequel, P., and Kayogoma, E., 2004, The making of the East African Craton (2.93–2.53 Ga): Orleans, Abstracts 20th Colloquium of African Geology, p. 336.

Porada, H., and Berhorst, V., 2000, Towards a new understanding of the Neoproterozoic–Early Paleozoic Lufilian and Northern Zambezi Belts in Zambia and Democratic Republic of Congo: Journal of African Earth Sciences, v. 30, p. 727–771, doi: 10.1016/S0899-5362(00)00049-X.

Potrel, A., Peucat, J., Fanning, C.M., Auvray, B., Burg, J., and Caruba, C., 1996, 3.5 Ga old terranes in the West African Craton, Mauritania: The Geological Society of London, v. 153, p. 507–510, doi: 10.1144/gsjgs.153.4.0507.

Poudjom Djomani, Y.H., O'Reilly, S.Y., Griffin, W.L., and Morgan, P., 2001, The density structure of subcontinental lithosphere: Constraints on delamination models: Earth and Planetary Science Letters, v. 184, p. 605–621, doi: 10.1016/S0012-821X(00)00362-9.

Prendergast, M.D., 2004, The Bulawayan Supergroup: A late Archaean passive margin-related large igneous province in the Zimbabwe craton: The Geological Society of London, v. 161, p. 431–445.

Priestley, K., McKenzie, D., and Debayle, E., 2006, The state of the upper mantle beneath southern Africa: Tectophysics, v. 416, p. 101–112, doi: 10.1016/j.tecto.2005.11.024.

Raith, J.G., Cornell, D.H., Frimmel, H.E., and de Beer, C.H., 2003, New insights into the geology of the Namaqua Tectonic Province, South Africa, from ion probe dating of detrital and metamorphic zircon: The Journal of Geology, v. 111, p. 347–366, doi: 10.1086/373973.

Ramokate, L.V., Mapeo, R.B.M., Corfu, F., and Kampunzu, A.B., 2000, Proterozoic geology and regional correlation of the Ganzi-Makunda area, western Botswana: Journal of African Earth Sciences, v. 30, p. 453–466, doi: 10.1016/S0899-5362(00)00031-2.

Rampone, E., 2004, Mantle dynamics during Permo-Mesozoic extension of the Europe-Adria lithosphere: Insights from the Ligurian ophiolites: Periodico di Mineralogia, Special Issue 1, v. 73, p. 215–230.

Rampone, E., Romairone, A., Abouchami, W., Piccardo, G.B., and Hofmann, A.W., 2005, Chronology, petrology and isotope geochemistry of the Erro-Tobbio peridotites (Ligurian Alps, Italy): Records of late Paleozoic lithospheric extension: Journal of Petrology, v. 46, p. 799–827, doi: 10.1093/petrology/egi001.

Renka, R.J., 1988, Multivariate interpolation of large sets of scattered data: Association for Computing Machinery, Transactions on Mathematical Software, v. 14, p. 139–148, doi: 10.1145/45054.45055.

Ring, U., Kröner, A., and Toulkerides, T., 1997, Paleoproterozoic granulite-facies metamorphism and granitoid intrusions in the Ubendian-Usagaran Orogen of northern Malawi, east-central Africa: Precambrian Research, v. 85, p. 27–51, doi: 10.1016/S0301-9268(97)00028-4.

Ring, U., Kröner, A., Buchwaldt, R., Toulkeridis, Th., and Layer, P.W., 2002, Shear-zone patterns and eclogite-facies metamorphism in the Mozambique Belt of northern Malawi, east-central Africa: Implications for the assembly of Gondwana: Precambrian Research, v. 116, p. 19–56, doi: 10.1016/S0301-9268(01)00233-9.

Ritsema, J., and van Heijst, H., 2000, New seismic model of the upper mantle beneath Africa: Geology, v. 28, p. 63–66, doi: 10.1130/0091-7613(2000)28<63:NSMOTU>2.0.CO;2.

Ritsema, J., Ni, S., Helmberger, D.V., and Crotwell, H.P., 1998, Evidence for strong shear velocity reductions and velocity gradient in the lower mantle beneath Africa: Geophysical Research Letters, v. 25, p. 4245–4248, doi: 10.1029/1998GL900127.

Ritsema, J., van Heijst, H., and Woodhouse, J.H., 1999, Complex shear wave velocity structure imaged beneath Africa and Iceland: Science, v. 286, p. 1925–1928, doi: 10.1126/science.286.5446.1925.

Robb, L.J., Armstrong, R.A., and Waters, D.J., 1999, The history of granulite-facies metamorphism and crustal growth from single zircon U-Pb geochronology: Namaqualand, South Africa: Journal of Petrology, v. 40, p. 1747–1770, doi: 10.1093/petrology/40.12.1747.

Rudnick, R.L., McDonough, W.F., and O'Connell, R.J., 1998, Thermal structure, thickness and composition of continental lithosphere: Chemical Geology, v. 145, p. 395–411, doi: 10.1016/S0009-2541(97)00151-4.

Santos, J.O.S., Hartmann, L.A., Gaudette, H.E., Groves, D.I., McNaughton, N.J., and Fletcher, I.R., 2000, A new understanding of the provinces of the Amazon Craton based on integration of field mapping and U-Pb and Sm-Nd geochronology: Gondwana Research, v. 3, p. 453–488, doi: 10.1016/S1342-937X(05)70755-3.

Santos, J.O.S., Potter, P.E., Reis, N.J., Hartmann, L.A., Fletcher, I.R., and McNaughton, N.J., 2003, Age, source and regional stratigraphy of the Roraima Supergroup and Roraima-like outliers in northern South America based on U-Pb geochronology: Geological Society of America Bulletin, v. 115, p. 331–348, doi: 10.1130/0016-7606(2003)115<0331:ASARSO>2.0.CO;2.

Schandelmeier, H., Wipfler, E., Küster, D., Sultan, M., Becker, R., Stern, R.J., and Abdelsalam, M., 1994, Atmur-Delgo suture: A Neoproterozoic oceanic basin extending into interior of northeast Africa: Geology, v. 22, p. 563–566, doi: 10.1130/0091-7613(1994)022<0563:ADSANO>2.3.CO;2.

Schenk, V., Wegner, H., Appel, P., and Schumann, A., 2004, Pan-African granulite-facies reworking of Archean granulites in the West Nile region (Congo craton; Uganda): 20th Colloquium on African Geology, Abstracts volume 127, BRGM, Orleans, France, June 2–7.

Schlüter, T., 1997, Geology of East Africa: Berlin, Gebrüder Borntraeger, 484 p.

Schmitz, M.D., and Bowring, S.A., 2004, Lower crustal granulite formation during Mesoproterozoic Natal-Namaqua collisional orogenesis, southern Africa: South African Journal of Geology, v. 107, p. 261–284, doi: 10.2113/107.1-2.261.

Schumann, A., Barifaijo, E., and Geisler, T., 1999, Preliminary results on the origin of granitoid rocks of Eastern Uganda and around Kampala—Magmatic or metasomatic?: Journal of African Earth Sciences, v. 28, no. 4A, p. 71–72.

Schumann, A., Schenk, V., Kulyanyingi, P.K., Morelli, C., Barton, E., and Garbe-Schönberg, D., 2004, Evidence for the widespread occurrence of neo-Archean GGM-type granitoids in eastern Uganda: Orleans, Abstracts, 20th Colloquium of African Geology, p. 366.

Sebai, A., Stutzmann, E., Mantagner, J.-P., Sicilia, D., and Beucler, E., 2006, Anisotropic structure of the African upper mantle from Rayleigh and Love wave tomography: Physics of the Earth and Planetary Interiors, v. 155, p. 48–62, doi: 10.1016/j.pepi.2005.09.009.

Shillington, D.J., Holbrook, W.S., Tucholke, B.E., Hopper, J.R., Louden, K.E., Larsen, H.C., Van Avendonk, H.J.A., Deemer, S., and Hall, J., 2004, Data report: Marine geophysical data on the Newfoundland nonvolcanic rifted margin around SCREECH transect 2, *in* Tucholke, B.E., Sibuet, J.C., and Klaus, A., eds.: Proceedings of the Ocean Drilling Program, Initial reports, v. 210, p. 1–36.

Simmons, N.A., Forte, A.M., and Grand, S.P., 2006, Constraining mantle flow with seismic and geodynamic data: A joint approach: Earth and Planetary Science Letters, v. 246, p. 109–124, doi: 10.1016/j.epsl.2006.04.003.

Simmons, N.A., Forte, A.M., and Grand, S.P., 2007, Thermochemical structure and dynamics of the African superplume: Geophysical Research Letters, v. 34, doi: 10.1029/2006GL028009.

Sleep, N.H., Ebinger, C.J., and Kendall, J.M., 2002, Deflection of mantle plume material by cratonic keels, *in* Fowler, C.M.R., Ebinger, C.J., and Hawkesworth, C.J., eds., The early Earth: Physical, chemical, and biological development: The Geological Society of London, Special Publication, v. 199, p. 135– 150.

Sobolev, S.V., and Babeyko, A.Y., 2005, What drives orogeny in the Andes?: Geology, v. 33, p. 617–620.

Stein, M., and Hoffmann, A.W., 1994, Mantle plumes and episodic crustal growth: Nature, v. 372, p. 63–68, doi: 10.1038/372063a0.

Stern, R.J., 1994, Arc assembly and continental collision in the Neoproterozoic East African Orogen: Implications for the consolidation of Gondwanaland: Annual Review of Earth and Planetary Sciences, v. 22, p. 319–351.

Tack, L., Fernandez-Alonso, M., Tahon, A., Wingate, M., and Barritt, S., 2002, The "Northeastern Kibaran Belt" (NKB) and its mineralisation reconsidered: New constraints from a revised lithostratigraphy, a GIS compilation of existing geological maps and a review of recently published as well as unpublished igneous emplacement ages in Burundi: Windhoek, Namibia, Extended Abstracts, 11th Quadrennial International Association on the Genesis of Ore Deposits Symposium and Geocongress 2002, p. 42.

Tahon, A., Fernandez-Alonso, M., Tack, L., and Barritt, S.D., 2004, New insights about the evolution of the Mesoproterozoic Northeastern Kibaran belt (Central Africa): Orleans, Abstracts, 20th Colloquium of African Geology, p. 389.

Taylor, S.R., and McLennan, S.M., 1985, The continental crust: Its composition and evolution: Oxford, Blackwell, 312 p.

Tchameni, R., Mezger, K., Nsifa, N.E., and Pouclet, A., 2000, Neoarchean crustal evolution in the Congo Craton: Evidence from K rich granitoids of the Ntem Complex, southern Cameroon: Journal of African Earth Sciences, v. 30, p. 133–147, doi: 10.1016/S0899-5362(00)00012-9.

Thomas, R.J., Eglington, B.M., Bowring, S.A., Retief, E.A., and Walraven, F., 1993, New isotope data from a Neoproterozoic porphyritic granitoid-charnockite suite from Natal, South Africa: Precambrian Research, v. 62, p. 83–101, doi: 10.1016/0301-9268(93)90095-J.

Thomas, R.J., Chevallier, L.P., Gresse, P.G., Harmer, R.E., Eglington, B.M., Armstrong, R.A., de Beer, C.H., Martini, J.E.J., de Kock, G.S., Macey, P.H., and Ingram, B.A., 2002, Precambrian evolution of the Sirwa window, Anti-Atlas Orogen, Morocco: Precambrian Research, v. 118, p. 1–57, doi: 10.1016/S0301-9268(02)00075-X.

Toteu, S.M., van Schmus, W.R., Penaye, J., and Michard, A., 2001, New U-Pb and Sm-Nd data from north-central Cameroon and its bearing on the pre-Pan African history of central Africa: Precambrian Research, v. 108, p. 45–73, doi: 10.1016/S0301-9268(00)00149-2.

Toteu, S.F., Penaye, J., Tchameni, R., and Van Schmus, W.R., 2003, Extension and evolution of the 2.1 Ga West-Central African belt in Camerun: European Geophysical Society, Geophysical Research Abstracts, v. 5, p. 11554.

Van Avendonk, H.J., Holbrook, W.S., Nunes, G.T., Shillington, D.J., Tucholke, B.E., Louden, K.E., Larsen, H.C., and Hopper, J.R., 2005, Seismic velocity structure of the Newfoundland rifted margin: Evidence for thinned continental crust, unroofed mantle and slow-spreading oceanic crust: Eos (Transactions, American Geophysical Union), v. 86, no. 52, Fall Meeting Supplement, Abstract T43B-1389.

van der Lee, S., and Nolet, G., 1997, Upper mantle velocity S structure of North America: Journal of Geophysical Research, v. 102, p. 22,185–22,838.

Vinyu, M.L., Hanson, R.E., Martin, M.W., Bowring, S.A., Jelsma, H.A., Krol, M.A., and Dirks, P.H.G.M., 1999, U-Pb and $^{40}Ar/^{39}Ar$ geochronological constraints on the tectonic evolution of the easternmost part of Zambezi orogenic belt, northeast Zimbabwe: Precambrian Research, v. 98, p. 67–82, doi: 10.1016/S0301-9268(99)00039-X.

Walraven, F., and Rumvegeri, B.T., 1993, Implications of whole-rock Pb-Pb and zircon evaporation dates for the early metamorphic history of the Kasaï craton, southern Zaïre: Journal of African Earth Sciences, v. 16, p. 395–404, doi: 10.1016/0899-5362(93)90098-B.

Weeraratne, D.S., Forsyth, D.W., Fischer, K.M., and Nyblade, A.A., 2003, Evidence for an upper mantle plume beneath the Tanzanian craton from Rayleigh wave tomography: Journal of Geophysical Research, v. 108, B9, doi: 10.1029/2002JB002273.

Wittlinger, G., and Farra, V., 2007, Converted waves reveal a thick and layered tectosphere beneath the Kalahari super-craton: Earth and Planetary Science Letters, v. 254, p. 404–415, doi: 10.1016/j.epsl.2006.11.048.

Woolley, A.R., 1987, Alkaline rocks and carbonatites of the world, Volume 3: London, British Museum (Natural History), 335 p.

Xu, X., O'Reilly, S.Y., Griffin, W.L., and Zhou, X., 2000, Genesis of young lithospheric mantle in southeastern China: A LAM-ICPMS trace element study: Journal of Petrology, v. 41, p. 111–148, doi: 10.1093/petrology/41.1.111.

Yibas, B., Reimold, W.U., Armstrong, R., Koeberl, C., Anhaeusser, C.R., and Phillips, D., 2002, The tectonostratigraphy, granitoid geochronology and geological evolution of the Precambrian of southern Ethiopia: Journal of African Earth Sciences, v. 34, p. 57–84, doi: 10.1016/S0899-5362(01)00099-9.

Zheng, J., Griffin, W.L., O'Reilly, S.Y., Zhang, M., Pearson, N.J., and Luo, Z., 2006, The lithospheric mantle beneath the southern Tianshan area, NW China: Contributions to Mineralogy and Petrology, v. 151, p. 457–479, doi: 10.1007/s00410-006-0071-x.

Manuscript Received 31 March 2008
Revised Manuscript Received 18 September 2008
Manuscript Accepted 25 October 2008